Received: 17 October 2023 | Revised: 2 July 2024 | Accepted: 12 July 2024

DOI: 10.1002/dep2.305

The Depositional Record
Open Access
A journal of the International Association of Sedimentologists
IAS
WILEY

ORIGINAL ARTICLE

Cretaceous cyclic peritidal carbonates of the Apulia Carbonate Platform (Apulia, southern Italy) in a hierarchical sequence-stratigraphic perspective: A case study from the Murge area (the Giovinazzo sea-cliff section)

Luigi Spalluto | **Marco Petruzzelli** | **Luisa Sabato** | **Marcello Tropeano**

Department of Earth and Geoenvironmental Sciences, University of Bari Aldo Moro, Bari, Italy

Correspondence
Luigi Spalluto, Department of Earth and Environmental Sciences, University of Bari Aldo Moro, via E. Orabona 4, Bari 70125, Italy.
Email: luigi.spalluto@uniba.it

Funding information
Universita degli Studi di Bari Aldo Moro; PRIN Project 2022 "Abrupt Lithofacies Variations IN the stratigraphic record: proxies for environmental and climate changes - ALVIN", Grant/Award Number: 2022APF9M2

Abstract

Cretaceous cyclic peritidal carbonates form the bulk of the Apulia Region in Italy and represent the vestiges of the Apulia Carbonate Platform. To show from a sequence stratigraphic perspective the architecture of peritidal carbonates, the 17 m thick Albian Giovinazzo sea-cliff section was studied at a centimetre detail, aiming to: (i) describe cyclic facies organisation in beds and bedsets; (ii) reconstruct the relative sea-level curve and its evolution over time; (iii) interpret the long-term evolution of the accommodation space in terms of sequence stratigraphy. The hierarchical stacking pattern of facies in beds and bedsets reveals Milankovitch cyclicity. As a working hypothesis, elementary sequences are assumed to represent the precession cycle (*ca* 20 kyr) and small-scale and medium-scale sequences the short (*ca* 100 kyr) and long (*ca* 400 kyr) eccentricity cycles, respectively. Four different types of elementary sequences (condensed, catch-down, catch-up and give-up) are recognised and interpreted in terms of relative sea-level changes to reconstruct the relative sea-level curve of the entire succession. The envelope of the reconstructed relative sea-level curve is used to represent the long-term accommodation change on the platform, which covers a time span of approximately 1.8 Myr. Most of this time was spent in subaerial exposure, as approximately 1.2 Myr was predicted to be condensed in a stratigraphic interval encompassing both the sequence-boundary zone/falling stage deposits and the lowstand deposits. Moreover, it was interpreted that about two-third of the total thickness of the succession was formed in only 280 kyr and consisted of both transgressive and maximum-flooding deposits. The main implication of this study is that unconformities do not necessarily correspond to single surfaces but, rather, to very amalgamated intervals or unconformity zones. Moreover, based on biostratigraphic constraints, there is a correlation between the unconformity

zone of the studied succession and the third-order KAl4 sequence boundary of the Cretaceous eustatic cycle chart.

KEYWORDS

accommodation space, Albian, Calcare di Bari Formation, peritidal facies, relative sea-level change, unconformity zone

1 | INTRODUCTION

Micrite-rich limestones and dolostones deposited on tidal flats and shallow lagoons form characteristic carbonate facies in tropical-type shallow marine depositional systems (see standard facies belts 7, 8 and 9 in Wilson, 1975; Flügel, 2004; Schlager, 2005). These facies are often indicated with the adjective 'peritidal' and correspond to the tidal-influenced, low-energy inner sector of a carbonate platform developed in the lee of rocky islands, pits, reefs or sand shoals (Pratt, 2010). In such a context, the threefold environmental subdivision is typically constituted by supratidal, intertidal and subtidal environments, in which the fine-grained carbonate facies show almost recurrent and easily recognisable sedimentary and early diagenetic features (Tucker & Wright, 1990; Demicco & Hardie, 1994). Although peritidal facies invariably develop in the tidal zone, the tides alone are too small to have a significant influence on sediment deposition. Rather, most of the sediment is transported by high winds, storms and hurricanes which stir up the subtidal environment forcing sediment-rich waters onto the tidal flat (Jones & Desrochers, 1992; Pratt, 2010). At low latitude, the carbonate factory is productive mostly in the permanently submerged subtidal environment where bioturbated and pelleted lime muds are variably rich in skeletal material stemming from benthic organisms such as gastropods, bivalves, benthic foraminifera, ostracods and green algae (T factory sensu Schlager, 2005). The intertidal environment is alternatively exposed and submerged and represents a low-energy and low-relief repository of allochthonous calcareous particles, born in the subtidal carbonate factory, which can remain trapped in the mucilage of microbial mats (Demicco & Hardie, 1994). Due to its almost flat morphology, the tidal flat may extend over large areas, even in microtidal settings, and is cut by tidal channels or creeks that drains the ebb tide (Shinn et al., 1969; Hardie, 1977). The supratidal environment lies above normal high-tide and is flooded only during spring tides, high winds and storms. This zone is mostly characterised by desiccation cracks and may be dotted by brackish ponds, in humid climates or by sabkhas, in arid climates (Assereto et al., 1977; Shinn, 1983; Martin-Chivelet & Gimenez, 1992). Depending on the degree and time of exposure, this zone may be also affected by pedogenesis (Enos, 1983; Wright, 1994, 1996; Azeredo et al., 2015).

A peculiar feature of peritidal carbonates is the ability to build kilometre-thick successions of repeated sequences in which metre-scale, asymmetric shallowing-upward cycles are the most commonly, but not exclusively, observed motif. Typically, these peritidal cycles show subtidal facies at the bottom that gradually pass upward to intertidal and supratidal facies. This peculiar feature was recognised elsewhere in the sedimentary record of carbonate successions formed along passive margins and for different geological time intervals. In such a context, the cyclical formation of accommodation space, that is, the result of the sum of subsidence and sea-level changes, was almost completely filled by peritidal carbonates through aggradation and/or regional progradation (Pratt, 2010). The asymmetry is related to the delay in restarting the subtidal carbonate factory after the subaerial exposure, since carbonate-dwelling biota first have to recolonise the exposure surface (lag time sensu Tipper, 1997). Although the stacking pattern of peritidal sequences gives rise to apparently monotonous and easily depictable successions of beds and bedsets in which facies features are continuously repeated, the interpretation of their origin has divided and still divides carbonate sedimentologists (see discussions in Eberli, 2013; Strasser, 2018). The stratigraphic record of peritidal facies is commonly seen as the spatio-temporal response to concomitant autogenic and allogenic forcing factors, where the separation of relative contributions is not always an easy task (Eberli, 2013; Strasser, 2018). Basically, autogenic factors are intrinsic to the depositional system and respond to random and unpredictable processes; whereas allogenic factors respond to external factors and are potentially predictable. According to the autogenic model, the sediment production and accumulation depend on the ecological characteristics of the carbonate factory, and by local hydrographic processes such as tides, winds and storms. Thus, shallowing-upward cycles represent a sediment body that has passively filled its available accommodation space and has aggraded from the subtidal

environment to beyond high-tide. This model assumes that sea level did not change during accommodation. Simply, given sufficient sediment supply, the tidal flat may migrate laterally over the adjacent lagoon forming asymmetric peritidal cycles (peritidal autocycles sensu Ginsburg, 1971). This implies that the cyclic stratigraphic pattern is deceptive, irregular and unordered because it is the result of a random combination of accretion, interruption, reworking, migration and drowning. As a result, deepening and shallowing trends in vertical facies stacking patterns are not related to relative sea-level changes but are just the result of stochastic processes (Eberli, 2013). The autogenic model seems to be the most reasonable interpretation when the lateral extent of peritidal facies cannot be determined and when stratigraphic distribution of facies appears statistically random. However, an important subsidence rate and/or a long-term sea-level rise are needed to create enough accommodation to accumulate a thick sedimentary record. It was demonstrated in several case studies, that the architecture of some platforms consists of laterally continuous, hierarchically bundled sequences where facies changes imply deepening-shallowing trends. These sequences are mostly ascribed to 4th and 5th order sequences (parasequences sensu Van Wagoner et al., 1988 or simple sequences sensu Vail et al., 1991) and their bounding surfaces correspond to sequence boundaries (Strasser et al., 1999). This kind of cyclicity requires extrinsic 'allogenic' forcing to be fully explained. In many cases, independent chronostratigraphic tie points suggest that the periodicity of shallowing-upward cycles, and their bundling into higher order cycles, may reflect the 20, 100 and 400 kyr Mikankovitch cycles, which correspond to precession, short eccentricity and long eccentricity orbital cycles respectively (D'Argenio et al., 1997, 1999, 2004; Strasser et al., 1999 among many others). Allogenic factors include either regional tectonic mechanisms, like the rate of subsidence, or global eustatic sea-level change, or both. If allocycle thickness is random and not bundled, then a tectonic control could appear to be dominant over eustacy (Bosence et al., 2009).

This paper is focussed on a 17 m thick shallow-water carbonate succession cropping out along the sea-cliff of the town of Giovinazzo in northern Murge (Apulia, southern Italy) (Figure 1). The goals of this paper are: (i) to propose a depositional model for the studied shallow-water carbonate succession based on a detailed facies analysis (centimetre-scale sampling); (ii) to describe in detail the facies stacking pattern in beds and bedsets in order to individuate elementary depositional sequences and their bundling; (iii) to interpret, according to the paradigms of sequence stratigraphy, both the short-term and long-term evolution of carbonate sedimentation in this sector of the Apulia Carbonate Platform (ACP) and (iv) to propose a tentative correlation between the large-scale evolution individuated in this study with the most recent Cretaceous global sea-level curve (Haq, 2014).

2 | GEOLOGICAL SETTING

The studied succession crops out in the northern part of the Murge area (Apulia, southern Italy) and belongs to the Calcare di Bari Formation (Figure 1). The Murge area is part of the extensive and only weakly deformed foreland area of both the Apennines and Dinarides-Albanides-Hellenides orogens: that is, the Apulian Foreland (Selli, 1962; Ricchetti et al., 1988; Figure 1). The sedimentary bulk of the Apulian Foreland is made up of a 6–7 km thick Mesozoic shallow-water carbonate succession developed on a large intra-oceanic platform not affected by terrigenous input: that is, the ACP (D'Argenio, 1974). During the Cretaceous, this platform was situated at a palaeolatitude of 20–25°N, along the southern margin of the Tethys Ocean (Stampfli & Hochard, 2009), and was part of the continental Adria Plate (Figure 2A). According to Nicolai and Gambini (2008), the ACP had an approximately N-S elongation with a length of about 650 km and a width of about 175 km, although its western boundary, buried under the southern Apennines chain, has never been identified. Although the ACP has been assimilated to a tropical-type carbonate platform having a modern analogue in the Bahamas (Eberli et al., 2004), the discoveries of several dinosaur footprints on some subaerially exposed surfaces have suggested an alternative palaeogeographical scenario that requires a connection, through land bridges or corridors, with continental areas (Bosellini, 2002; Zarcone et al., 2010; Petti et al., 2018, 2022; Antonelli et al., 2023; Figure 2B).

The ACP started to be an independent platform since the Early Jurassic rifting phase that affected the diverging Eurasia and African plates, breaking up a pre-existing epeiric platform (southern Tethys megaplatform sensu Vlahovic et al., 2005) in alternating shallow and deep-water domains. The vestiges of these domains crop out in the present-day peri-Adriatic area (Zappaterra, 1990). Most of the outcropping ACP shallow-water carbonate succession is exposed in the Apulian foreland (Gargano, Murge and Salento) with a maximum thickness of about 3000 m in the Murge area (Ricchetti, 1975), which covers a large part of the Cretaceous (from the Valanginian to the Maastrichtian according to Ciaranfi et al., 1988; Luperto Sinni, 1996 and Spalluto et al., 2005). The oldest part of this succession dates back to the middle and late Jurassic and crops out in the western Gargano Promontory (Spalluto et al., 2005; Spalluto & Pieri, 2008). The impressive

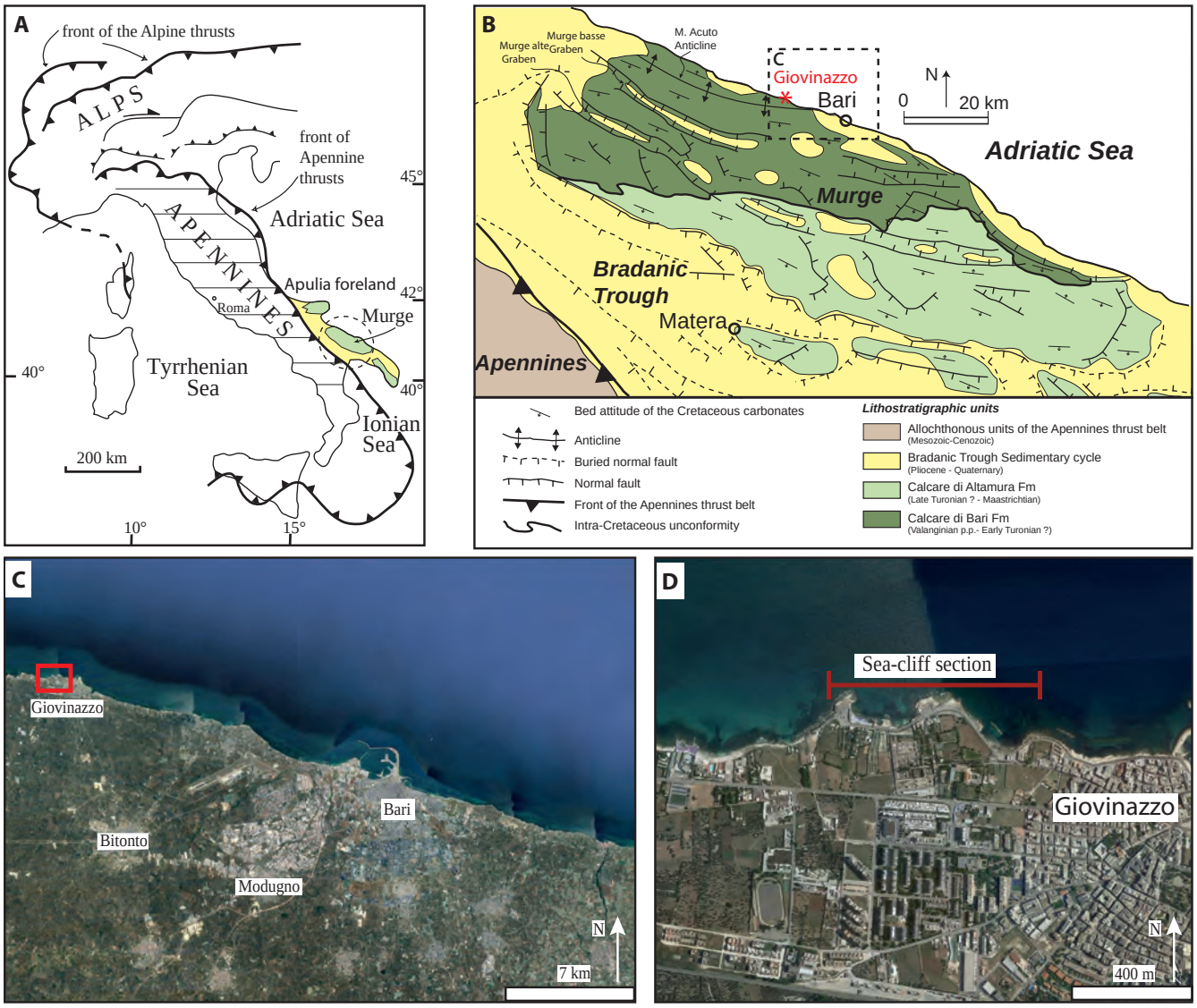

FIGURE 1 (A) Location of the Apulia foreland in a simplified structural map of Italy. (B) Geological map of the Murge area with location of the study area (red asterisk). (C) Geographic setting of the northern Murge with location of Giovinazzo town. The red rectangle indicates the area shown in inset (D). (D) location of the sea-cliff section along the coast of Giovinazzo town.

succession of parallel-bedded limestones was only temporarily interrupted by an intra-Cretaceous tectonically enhanced unconformity marked by bauxites, terra rossa and clayey terrestrial deposits formed in the Turonian during a prolonged (about 4 Myr) subaerial exposure of the platform (Crescenti & Vighi, 1964). The shallow-marine carbonate succession was described as a monotonous peritidal and shallow subtidal succession where biotically-controlled sedimentation easily balanced local subsidence rates (Ricchetti, 1975; Ciaranfi et al., 1988). The basic building blocks of the Cretaceous carbonate succession are well-developed asymmetrical, shallowing-upward, peritidal metre-scale cycles. The postulate of this observation-based model was that sedimentation rates were high enough to fill the whole accommodation space, forming shoaling autocycles in shallow-water environments (Ricchetti, 1975). Recent studies, based on detailed facies analysis at a centimetre-scale and on stable isotopes, have introduced a more complex scenario in which important, global-scaled climate changes played an important role in regulating the stacking patterns of facies as well as carbonate productivity (Spalluto, 2008, 2012; Graziano, 2013; Graziano et al., 2013).

3 | MATERIALS AND METHODS

The Giovinazzo sea-cliff section is well-exposed along the Adriatic coast of the northern Murge (Apulia, southern Italy; Figure 1D). Unfortunately, following the recent works to protect the sea front from coastal erosion, it is now partly covered by a retaining wall. The section

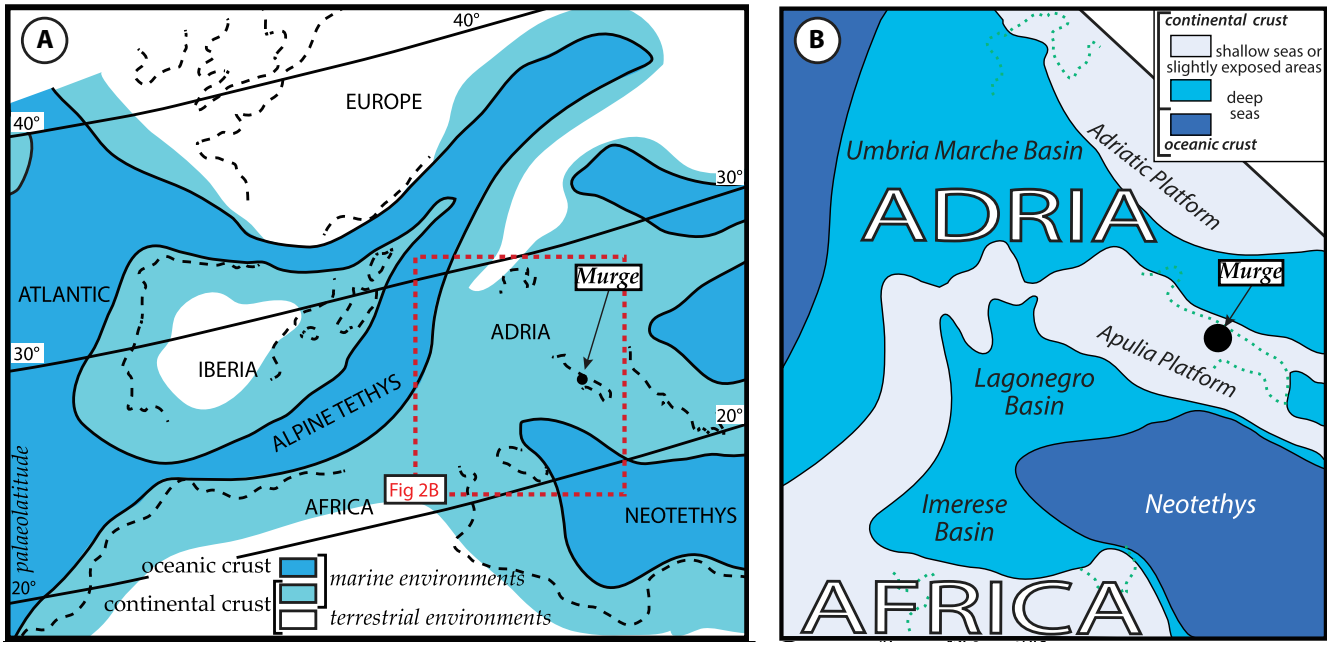

FIGURE 2 (A) Palaeogeographical map of Adria during Albian/Cenomanian times. Modified from Tropeano et al. (2023) after Stampfli and Hochard (2009). (B) Palaeogeographical map modified from Tropeano et al. (2023) after Patacca and Scandone (2013).

was previously investigated by Gallo Maresca (1994) for rudist assemblages, by Spalluto and Caffau (2010) for lithostratigraphy, biostratigraphy and chronostratigraphy, by Spalluto et al. (2008) and Spalluto (2012) for facies analysis and sequence chronostratigraphy.

The section has been logged and sampled at a centimetre-scale. Facies features were described in the field using a 10× hand lens and in 40 thin sections using a polarised optical microscope Nikon E600 POL. Facies were analysed in the field and under optical microscope using the Dunham (1962) classification scheme, as modified by Embry and Klovan (1971) and providing a semi-quantitative estimation of the abundance of carbonate grains. Special attention was paid to the detection of sedimentary structures and discontinuity surfaces. The set of sedimentological information was used to interpret the depositional environments (Wilson, 1975; Flügel, 2004). Subsequently, the observed repetitive facies stacking patterns were interpreted following a cyclostratigraphic approach (Strasser et al., 2006). The adopted nomenclature is that proposed by Strasser et al. (1999) and following studies for Milankovitch-driven, high-frequency sequences found in shallow-water carbonate successions. Therefore, the term 'sequence' is preferred to 'cycle' to indicate all transgressive-regressive deposits, regardless of their thickness and duration, formed under the influence of cyclical processes, including relative sea-level changes (Strasser, 2018). Consequently, the relative sea-level curve (i.e. the combined product of eustasy and tectonic subsidence) was reconstructed based on the interpretation of the different types of elementary sequences in terms of different amplitudes of high-frequency relative sea-level changes. The relative sea-level curve was then plotted in a time framework under the working hypothesis that each elementary sequence formed in a time interval of 20 kyr (precession cycle). The position of 'missed beats' (i.e. the missed record of elementary sequences due to subaerial exposure sensu Goldhammer et al., 1990) was also proposed based on the cyclostratigraphic interpretation. Finally, the long-term relative-sea level curve (i.e. the curve obtained by the envelope of high-frequency sea-level fluctuations) allowed the sedimentary record to be interpreted in terms of sequence stratigraphy.

4 | RESULTS

4.1 | Lithostratigraphy

The studied succession is about 17 m thick and can be divided into two different intervals (Figure 3). The lower interval is about 6 m thick and shows well-defined beds. Bed thicknesses vary between 0.10 and 0.65 m. Limestones are mostly mud-supported, corresponding to calcilutites (mudstones and wackestones), stromatolites and to very fine peloidal calcarenites (packstones) with a poorly differentiated microfossiliferous assemblage, in which small-sized benthic foraminifers, calcareous algae and ostracods prevail. Macrofossils are rare and consist of gastropods and bivalve fragments. Some beds show pervasive bioturbation due to the occurrence of root traces that typically start from the bed surfaces and penetrate deep into the

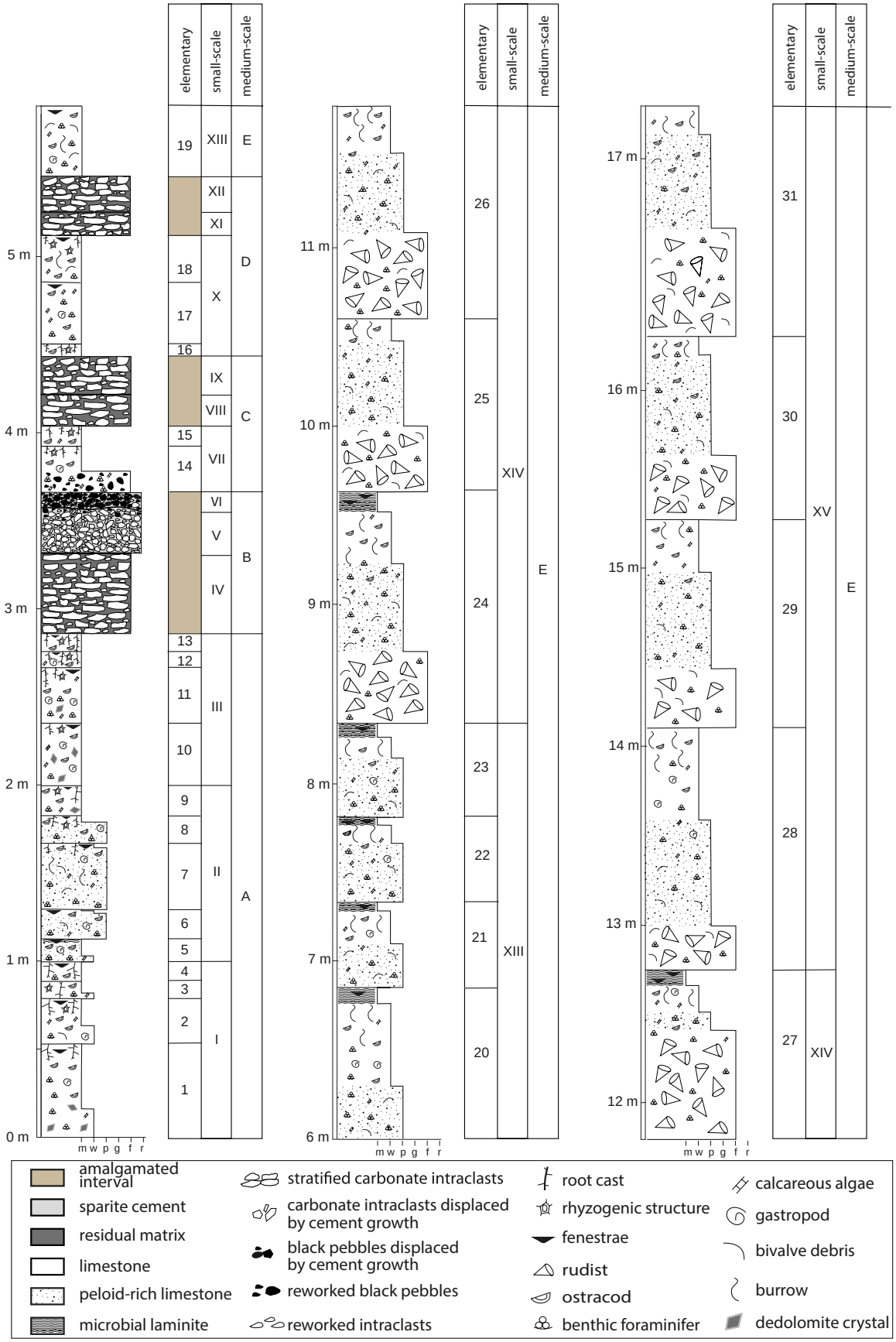

FIGURE 3 Stratigraphic log of the Giovinazzo sea-cliff section showing facies features and the cyclostratigraphic interpretation (see Section 4 for details). Modified Dunham classification: Mudstone (m), wackestone (w), packstone (p), grainstone (g), floatstone/rudstone (f/r) and bindstone (b). Note that arab numbers 1-31 correspond to elementary sequences; roman numbers I-XV correspond to small-scale sequences; capital letters A-E correspond to medium-scale sequences.

underlying limestones. In the upper part of this interval, these lithologies alternate with three distinct brecciated layers showing a residual clayey-silty yellowish or greenish matrix. Within each brecciated layer, faint bed surfaces may be individuated, indicating that each breccia layer was not the result of a single episode but, more likely, the result of the amalgamation of multiple events of limestone deposition and brecciation. Clasts are mostly pebble-sized and consist of the same lithologies as the underlying, not brecciated, beds. Some clasts are blackened (black pebbles); these latter are mostly found concentrated at the top of the first brecciated layer. Brecciated layers show a lateral continuity that covers the whole extent of the outcrop (>30 m; Figure 4).

The upper interval is about 11 m thick and is characterised by the occurrence of rudist-rich beds. Beds are significantly thicker than in the first interval, ranging between 0.5 and 1.5 m. Limestones are mostly grain-supported, corresponding to rudist-dominated medium to coarse-grained deposits. Rudists form decimetre to metre thick sheet-like tabular bodies, are laterally traceable, loosely packed (isolated) and the shells are whole, in growth position or more commonly randomly oriented (Figure 5). The matrix of the rudist-rich beds is composed of medium to coarse-grained bioclastic calcarenites with a relatively wide range of skeletal particles (mostly molluscs and benthic foraminifers). The following association of rudists characterises this interval (Gallo Maresca, 1994): *Eoradiolites murgensis*, *Eoradiolites lyratus*, *Apricardia* sp. This rudist association belongs to the 'Livello Palese' of the Calcare di Bari Formation (Ricchetti, 1975), which extensively crops out in the northern Murge representing a reference level for stratigraphic correlations at regional scale (Spalluto, 2012).

4.2 | Biostratigraphy

The time control of the studied succession is based on the stratigraphic distribution of benthic foraminifers. According to Spalluto and Caffau (2010), two associations were identified in the studied succession: the first association occurs in the lower interval of the studied succession, below the first breccia layer, and is defined by the concomitant occurrence of the following taxa: *Cuneolina sliteri*, *Cuneolina pavonia*, *Cuneolina parva*, *Praechrysalidina infracretacea*, *Sabaudia minuta*, *Novalesia angulosa*, *Nezzazatinella picardi*, *Nezzazata isabellae*, *Vercorsella arenata* and *Vercorsella scarsellai*. The association of these taxa supports an early Albian age according to Arnaud Vanneau and Sliter (1995) and Velić (2007). The second association occurs in the upper interval of the studied succession. It is defined by the concomitant occurrence of two main orbitolinid taxa: 'Valdanchella' *dercourti* and *Neoiraqia insolita*, which represent valid biostratigraphic markers. Associated fauna are *Paracoskinolina fleuryi*, *P. infracretacea*, *N. isabellae*, *N. picardi* and *C. parva*. This association supports a late Albian age following Husinec and Sokać (2006) and Velić (2007). In this regard, it should be noted that the cited biostratigraphic papers informally divide the Albian stage into early and late substages, without distinguishing the middle one. Consequently, the first occurrence of the orbitolinids found in the second association is crucial

FIGURE 4 Outcrop photograph of the lower part of the Giovinazzo sea-cliff section. Note the lateral continuity of the brecciated layers over the whole extent of the outcrop.

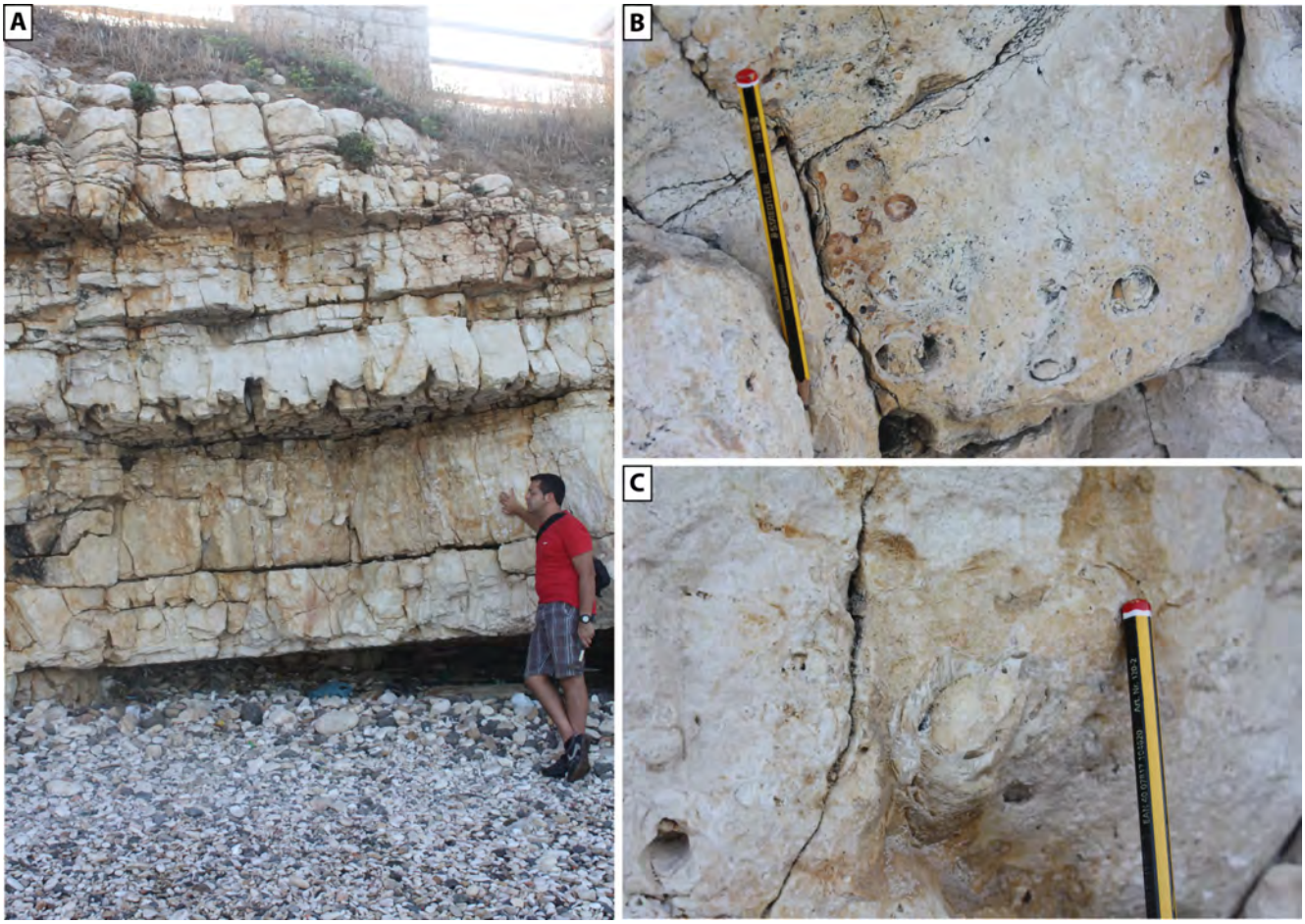

FIGURE 5 (A) Outcrop photograph of the upper part of the Giovinazzo sea-cliff section showing metre-thick rudist-rich beds. (B) Detail of a bed showing toppled rudists in a bioclastic matrix. (C) *Eoradiolites* sp.

for the chronostratigraphic attribution of the studied succession since it can be referred to the early late Albian (Husinec & Sokać, 2006; Velić, 2007). Furthermore, the last occurrence of *C. sliteri* and other taxa, below the three brecciated layers, is attributed to the latest lower Albian (Velić, 2007). This chronostratigraphic attribution is also confirmed by the radiolitid association of the 'Livello Palese' found in the rudist-rich beds of the upper interval. *Eoradiolites murgensis* and *E. lyratus* are widespread in upper Albian platform and slope successions of the ACP (Gallo Maresca, 1994; Luperto Sinni & Borgomano, 1994).

4.3 | Facies analysis

Facies analysis was performed both in the field and in thin section to recognise facies constituents, texture, fabric, early diagenetic overprint and fossil content. Six main facies have been distinguished representing as many subenvironments belonging to the inner platform domain. The facies analysis is described in detail below.

4.3.1 | Intraformational breccia

This facies occurs in three laterally continuous brecciated layers found in the lower part of the studied succession (Figure 3). Breccias mostly form chalky dense assemblages of pebble-sized subangular or subrounded clasts in a greenish or light brown silty-clayey matrix. They show extremely poor sorting, are arranged in sheet-like horizons that still preserve the relics of the original stratification and are not reworked. Limestone clasts show a strong compositional similarity with the limestone of the underlying beds. The lower part of the breccia layers grades downward into the underlying limestone rock through a transition zone showing strong evidence of in-situ alteration and brecciation (Figure 6A). Only the first of the three breccia layers shows an upper well-cemented part that, in the outcrop, stands out as a prominent feature since it is more resistant to weathering than the underlying one (Figure 6B). This latter is crossed by an irregular erosive surface. Above this surface, black pebbles become predominant and form a clast-supported dense dark horizon (Figure 6C). The intergranular pores of the well-cemented

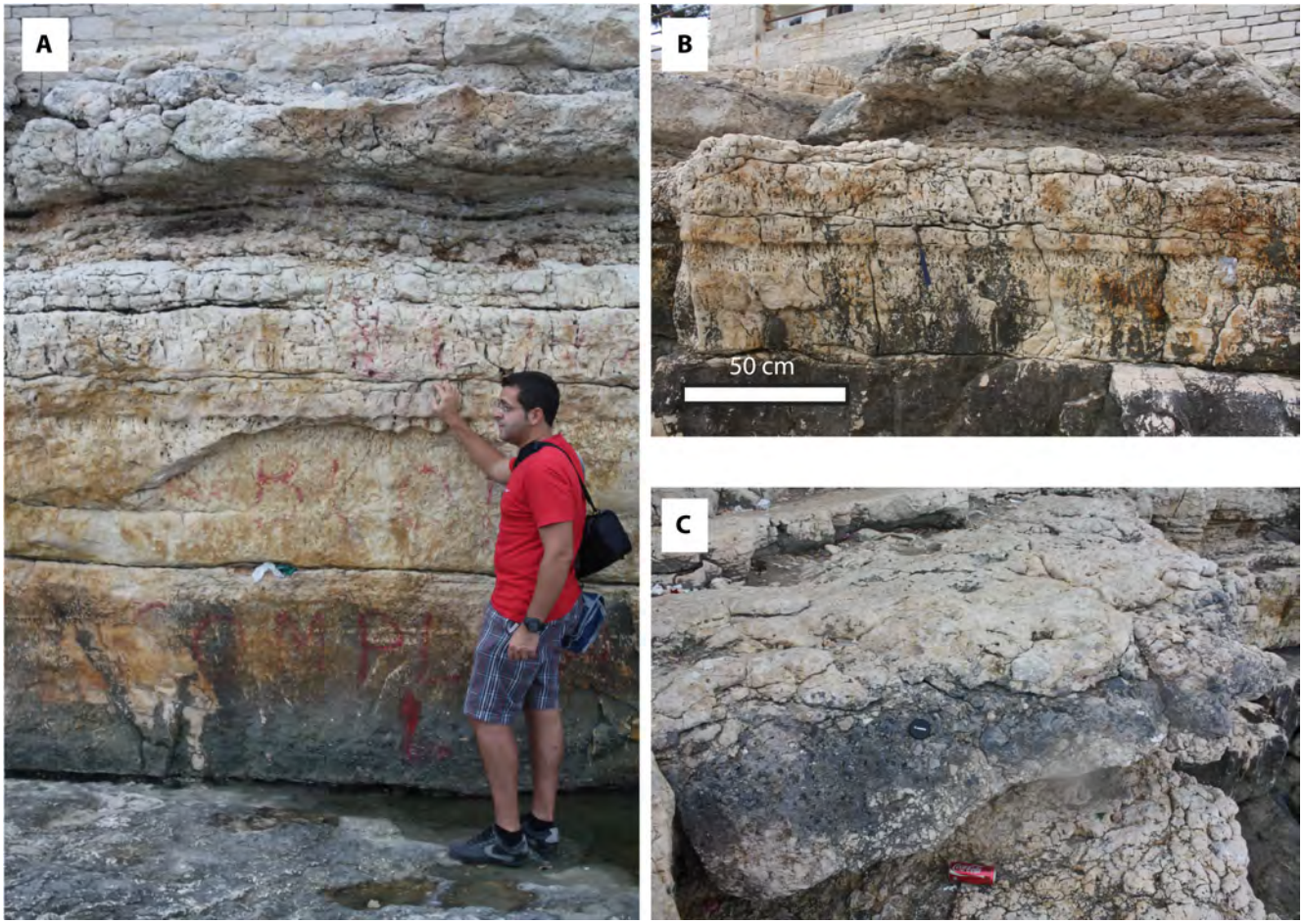

FIGURE 6 Outcrop photographs of the lower part of the study section. Note in (A) and (B): (i) gradual upward decrease in bed thicknesses (from 10 to 13 in Figure 3), which also corresponds to an increase in rhizoturbation; (ii) preservation of relics of the original stratification in the first brecciated layer (from IV to VI in Figure 3); (iii) the well-cemented upper part of the first brecciated layer (V and VI in Figure 3) protrudes from the outcrop since it is more resistant to weathering. Note in (C) the dark horizon formed by black pebbles in the uppermost part of the first brecciated layer (VI in Figure 3).

interval are commonly filled by matrix-replacive, fine to medium-grained, euhedral to subhedral dedolomite crystals forming an idiotopic to hypidiotopic mosaic texture (Figure 7A). Black pebbles may be also found reworked at the base of the overlying bed, embedded in a carbonate matrix.

Environmental interpretation

This facies is interpreted as having formed by in-situ brecciation, controlled by soil-forming processes in supratidal environments, of limestones previously deposited in the restricted subtidal zone. The chalky part may correspond to the early stage in the formation of a soil on carbonate rocks (Esteban & Klappa, 1983) and shows evidence of in-situ dissolution and partial replacement of the original material. Specifically, weathering produced both pervasive brecciation of the original limestone and accumulation of the residual silty-clayey detritus. The upper, well-cemented part may correspond to the mature stage in the formation of a soil since precipitation of calcium carbonate leads to the lithification and fossilisation of the soil profile and formation of a hardpan (Esteban & Klappa 1983). The presence of black pebbles confirms this interpretation since they are considered to be important markers for partial or complete subaerial exposure (Strasser & Davaud, 1983; Flügel, 2004) and frequently occur in carbonate soils (Esteban & Klappa, 1983).

4.3.2 | Laminated microbial bindstone

This facies consists of laminated microbial bindstone (sensu Demicco & Hardie, 1994) showing flat to wavy geometries (LLH stromatolites sensu Logan et al., 1964). At the thin section scale, it shows irregular and frequently discontinuous millimetre-thick laminae made up of peloids, micritic intraclasts, bivalve fragments, small-sized benthic foraminifers, *Thaumatoporella* sp. and ostracods.

The sediment is characterised by millimetre-sized fenestral cavities (Figure 7B). Fenestrae may form a network of laminoid or irregularly distributed spar-filled cavities. Desiccation cracks due to the shrinkage of the carbonate mud may be present at the top of this facies.

Environmental interpretation

Small-sized fenestrae found in microbial limestones have a polygenic origin and are preserved during the early stages of diagenesis. They may be caused by: (a) wetting and drying of carbonates in upper intertidal/lower supratidal environments (Shinn, 1968); (b) drying of cyanobacterial mats (Hardie & Shinn, 1986); (c) degassing of decaying organic material (Shinn, 1983). Although fenestral microbial bindstones may form in different environments, their occurrence together with early diagenetic desiccation features constrain the interpretation to upper intertidal/lower supratidal environments (Shinn, 1983; Berkeley & Rankey, 2012).

4.3.3 | Rhizoturbated pelleted mudstone/wackestone with fenestral fabric

This facies occurs only in the lower part of the studied succession and is predominantly made up of pelleted lime mudstones and wackestones in which only thin-shelled ostracods, miliolids, gastropods and micritic intraclasts may be recognised (Figure 7C). It has a typical mottled-grey colour and is rhizoturbated. Rhizoturbation is produced by a dense network of rootlets. Root casts may be unfilled, partly filled by internal sediment and dedolomite crystals or moulds, or enlarged by dissolution and filled by calcite (Figures 5A,B and 7D). The fenestral fabric consists of irregularly shaped voids (stromatactoid fabric) locally filled with fine-grained geopetal sediments (vadose silt sensu Dunham, 1969) at the base and sparry calcite at the top (Figure 7E). The upper part of the larger cavities may also show microstalactitic cements. Micritic intraclasts show circumgranular cracking (Figure 7F). Euhedral to subhedral dedolomite crystals are also widespread in this facies (Figure 7G). They are randomly sparse in the matrix or fill root casts and burrows, and typically show a thin rhomb-shaped crystalline rim with a micritic centre. Some rhombs may have one of more of their corner missing. Dolomoulds may also occur and show geopetal infillings similar to fenestrae (Figure 7H).

Environmental interpretation

Pelleted micrites without fossils or with reduced benthic biota are usually diagnostic of low-energy restricted shallow-lagoon environments characterised by critical values of temperatures and/or salinities and by oxygen depletion (Enos, 1983). The concomitant occurrence of fenestrae, root casts, dedolomite crystals and moulds suggests that, after deposition of lime muds, this facies experienced vadose diagenesis in supratidal environments (D'Argenio et al., 1997; Spalluto, 2012; Le Goff et al., 2015).

4.3.4 | Miliolid-ostracod-algal wackestone/packstone

This facies is mostly made up of strongly burrowed wackestones and subordinately packstones with benthic foraminifers (typical are miliolids, cuneolinids and textularids), ostracods, calcareous algae, requienids, gastropods, *Thaumatoporella* sp., small-sized oncoids, micritic intraclasts and peloids (Figure 8A). Biota show a reduced diversity but commonly with a high number of individuals. Usually, faecal pellets fill burrows (Figure 8B).

Environmental interpretation

Taking into account: (a) the limited number of grain types; (b) the absence of grain reworking, abrasion, rounding and sorting; (c) the reduced diversity of exclusively benthic biota but relatively great number of those few organisms adapted to survive; (d) the reduced size of individuals (dwarf fauna) and (e) the lack of desiccation structures and other features indicating tidal flat environment (e.g. microbial laminae and/or fenestrae), this facies is interpreted as deposited in low-energy semi-restricted shallow-subtidal environments (D'Argenio et al., 1997, 1999; Raspini, 1998, 2001; Spalluto, 2012).

4.3.5 | Biopeloidal packstone/grainstone

Description

This facies is made up of biopeloidal packstones/grainstones mostly made up of micritised aggregate grains in association with micritised skeletal grains (rudists and gastropods), micritic intraclasts, small-sized benthic

FIGURE 7 Thin section photomicrographs. (A) Intraclast floatstone showing matrix-replacive, medium-grained, euhedral to subhedral dedolomite rhombs forming an idiotopic to hypidiotopic mosaic texture. (B) Irregularly laminated microbial bindstone showing a well-developed fenestral fabric. (C) Pelleted mudstone showing a geopetally infilled fenestrae. Note also a gastropod mould filled by blocky calcite. (D) Cross-section of unfilled root casts in an inhomogeneous micrite. (E) Fenestral mudstone: Note the geopetal fabric consisting of dark vadose silt at the bottom and coarse calcite crystals at the top. (F) Circumgranular cracking around a micritic intraclast. (G) Dedolomite showing thin rhomb-shaped crystalline rims with micritic centres. Some rhombs are missing one or more corners. (H) Dolomoulds geopetally infilled by vadose crystal silt (near-surface early vadose dedolomitisation).

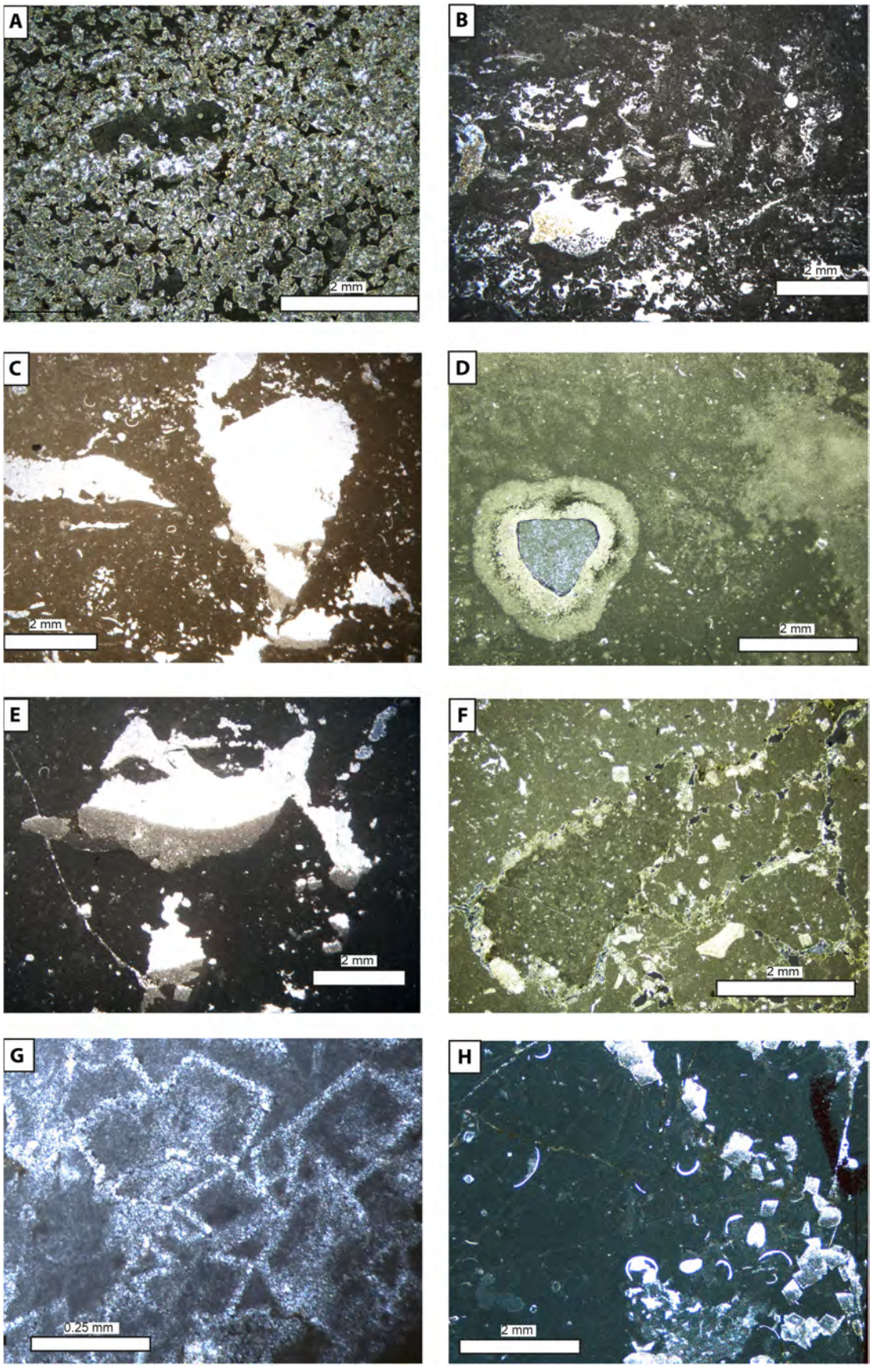

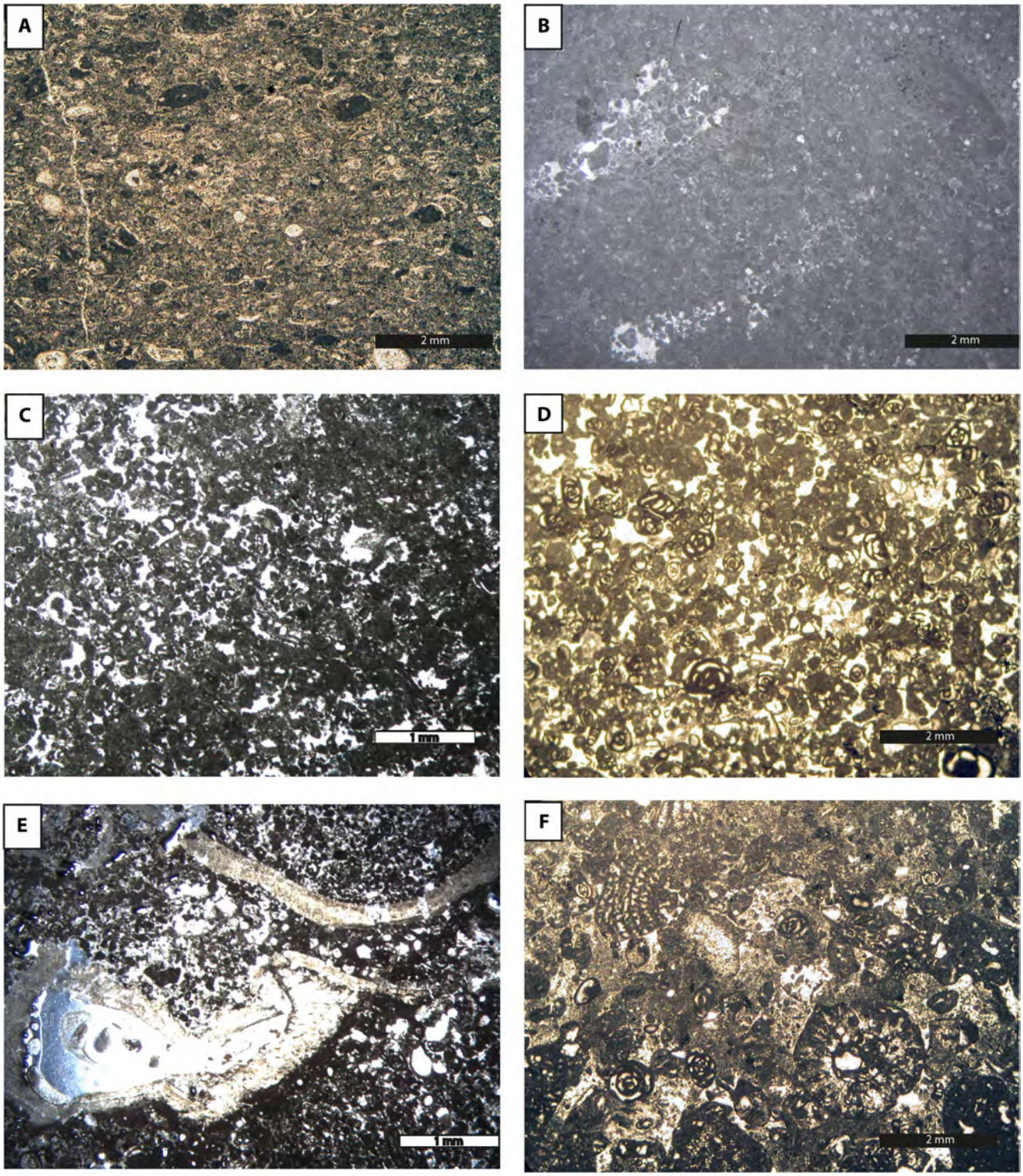

FIGURE 8 Thin section photomicrographs. (A) Wackestone made up of abundant ostracods and faecal pellets. (B) Burrowed wackestones made up of peloids, ostracods and small-sized miliolids. Note the faecal pellets filling the burrows. (C) Biopeloidal packstone mostly made up of micritised aggregate grains (lumps) in association with micritised skeletal grains, micritic intraclasts, small-sized benthic foraminifers, dasycladacean fragments, porostromate oncoid and peloids. (D) Detail of biopeloidal packstone showing some orbitolinid tests. (E) Rudist floatstone in a sand-sized bioclastic matrix. (F) Detail of rudist floatstone matrix showing abundant benthic foraminifers and green algae.

foraminifers, dasycladacean fragments, porostromate oncoids and peloids (Figure 8C,D). Aggregate grains consist predominantly of lumps, showing the characteristic lobate outline (grapestone), made up of small bioclasts and peloids bound together by microcrystalline calcite. Most grains show an isopachous rim of early-marine cement. Coarser crystals of equant calcite fill interparticle and intraparticle pores. Facies constituents are occasionally arranged in parallel to undulated laminations and show prevailingly normal gradation.

Environmental interpretation

The grain-supported textures, the presence of high-energy sedimentary structures and the normal grading of grains suggest that this lithofacies was deposited in shallow wave or current-agitated open lagoonal environments where migrating sandbars could form. The occurrence of a normal-marine and diversified benthic fauna also supports this interpretation (D'Argenio et al., 1997, 1999; Raspini, 1998, 2001; Spalluto, 2012).

4.3.6 | Rudist floatstone

Description

This facies is made up of mollusc-bearing floatstones in a bioclastic wackestone/packstone or packstone/grainstone matrix (Figure 8E). The dominant biota are rudists (mostly radiolitids and requienids) in association with gastropods. Rudist-dominated assemblages occur in sheet-like concentrations in which individuals are loosely packed and completely lack mutual support. Typically, rudist shells lack the upper valve and are in growth position or, more commonly, slightly oblique (with random orientation of tests). The coarse sandy matrix consists of skeletal fragments, which derived from bioerosion and mechanical breakdown of rudist shells, seldom showing a micritic envelope (cortoids). Associated are benthic foraminifers, fragments of dasycladacean algae and echinoids, solitary corals, grapestones and micritic intraclasts (Figure 8F). Peloids occur only rarely.

Environmental interpretation

The relatively high fossil diversity and abundance is consistent with deposition in normal-marine lagoonal environments under conditions of low to moderate water energy. These environments corresponded to rudist-inhabited sand plains, in which the main source of carbonate sediment is represented by the fragmentation of rudist shells (Carannante et al., 2000; Simone et al., 2003; Spalluto, 2012; Le Goff et al., 2015).

4.4 | Depositional sequences

In the studied section, the vertical organisation of facies in beds and bedsets shows a clear cyclic recurrence of both depositional and early diagenetic features. The smallest identifiable sequence corresponds to an elementary depositional sequence (sensu Strasser, 1991, 1994; Strasser et al., 1999). Elementary sequences represent the sedimentary record of the highest frequency relative sea-level change cycles and typically show an initial thin transgressive trend, followed by a thicker and much more well-developed regressive trend. Therefore, bed surfaces are interpreted to be the sequence boundaries of elementary sequences and normally correspond to surfaces that cap the shallowest facies of each bed (Strasser, 1994; D'Argenio et al., 1997). In such a context, lowstand deposits are lacking as there is no production and, consequently, no accumulation of carbonate sediment (Tipper, 1997; Kemp & Sadler, 2014). As a result, transgressive surfaces coincide with sequence boundaries. A lag of reworked intraclasts, including black pebbles, locally marks the early phases of the transgression. Transgressive deposits are thin or absent, and the deepest facies of each sequence lies directly above the underlying sequence boundary. Highstand deposits of elementary sequences are always well-developed and are indicated by the shallowing-upward facies trend.

According to their facies evolution, three main kinds of elementary sequences can be recognised (Figure 9). However, it should be noted that the brecciated layer shown in Figure 9A does not represent a fourth kind of sequence, but it is the result of the pedogenetic brecciation of a previously formed elementary sequence. Moreover, elementary sequences have not been identified in the brecciated layers, even if the relics of the original stratification may be observed. Therefore, excluding the brecciated layers from the count, 31 elementary sequences have been recognised in the studied section, each of which corresponds to a single bed (Figure 3). Summing up, the lower part of the section (from 1 to 19 in Figure 3) is made up of thin elementary sequences, from a few centimetres to about 50 cm thick, in which the shallowing upward trend is identified by vertical facies changes and by vadose diagenesis (fenestrae, desiccation cracks, circumgranular cracks) and weak pedogenetic features (rhizoturbation) affecting directly restricted subtidal facies without the interposition of intertidal facies (Figure 7A through H). Furthermore, rhizoturbation is pervasive in some elementary sequences as it crosses almost their entire thickness (sequences 2–4, 12–13, 15 and 16 in Figures 3 and 6A,B,C). These elementary sequences are here compared to base-cutout catch-down cycles (Soreghan & Dickinson, 1994; Hillgartner & Strasser, 2003). The base cutout is due to

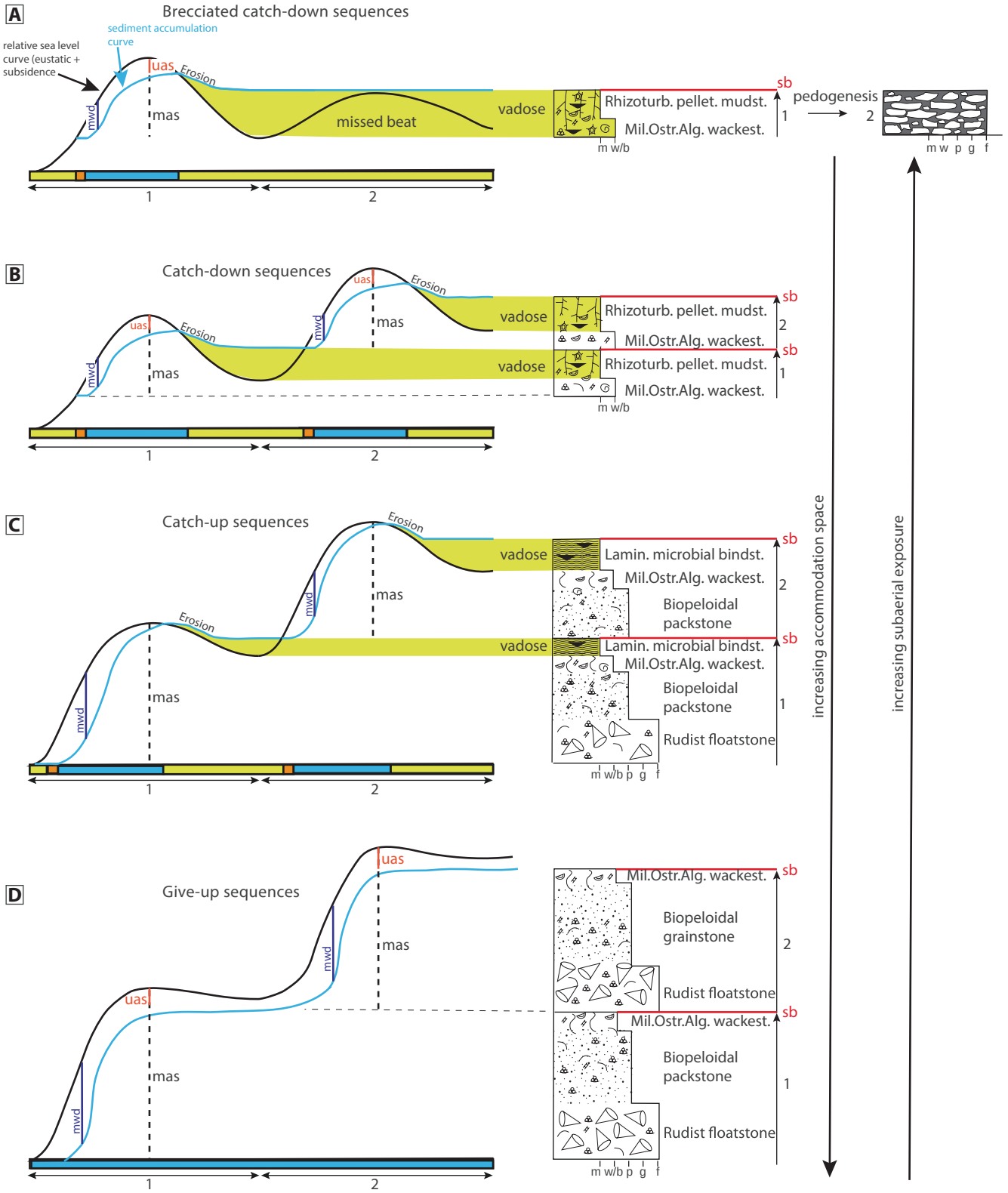

FIGURE 9 Conceptual model showing four different cases of facies evolution in elementary sequences reflecting variable sedimentation rates with respect to amplitude of relative sea-level changes (i.e. the sum of eustacy and subsidence). (A) Amalgamated sequences, (B) Catch-down sequences. (C) Catch-up sequences. (D) Give-up sequences. On the time axis, the blue bar indicates the time of carbonate production and accumulation; the yellow bar indicates the time of erosion and vadose diagenesis during subaerial exposure; the orange bar indicates the lag time required for the carbonate producing-biota to restart the factory after subaerial exposure. The adopted sequence nomenclature is from Soreghan and Dickinson (1994) and Hillgartner and Strasser (2003). For more explanation about sequences formation refer to the text.

evidence that shelf flooding occurs only in the late transgressive/early highstand phase of the relative sea-level curve (Figure 9B). Thereafter, sediment accumulation lags behind the initial creation of accommodation space, as demonstrated by the deposition of subtidal facies at the base of these sequences, but then overtakes falling sea level (i.e. the sediment accumulation curve intersects the relative sea-level curve on its falling leg in the late highstand), as shown by the gradual and uninterrupted shallowing-up facies evolution and, mostly, by the overprinting of early vadose fabric, developed in the meteoric regime of the supratidal area, directly atop the restricted subtidal facies (Figure 9B). Resultant sequences are then both thickness incomplete (i.e. sediment accumulation has not filled all the available accommodation space) and facies incomplete (i.e. intertidal facies are missing; Figure 9B). Regarding the brecciated layers, facies analysis revealed that they were originally formed in restricted subtidal environments and that the brecciation occurred subsequently due to prolonged subaerial exposure and pedogenesis. Although, as previously noted, no clear elementary sequences were delimited in these intervals, a twofold scenario may be proposed for interpreting the formation of the brecciated layers (Figure 9A). At first, relative sea-level rise was able to produce enough accommodation for the formation of a base-cutout catch-down elementary sequence, but a subsequent drop resulted in subaerial exposure of the whole thickness of the sequence and the development of pervasive vadose diagenesis. Afterwards, the amplitude of the subsequent relative sea-level rise was not sufficient to bring the exposed surface below sea level, that is, the highest point of the expected sediment accumulation curve does not lead to additional space for sediment in that area, resulting in no accumulation ('missed beat' sensu Goldhammer et al., 1990; Figure 9A). This explains the strong pedogenetic modification of the previously formed elementary sequence since the duration of the subaerial exposure was much longer than that assumed for the catch-down sequences (compare Figure 9A,B).

The upper part of the section shows two more types of elementary sequences. Elementary sequences 20–24 and 27 correspond to almost complete peritidal sequences since, from bottom to top, a gradual facies evolution from subtidal to supratidal deposits has been observed. These latter are the most described elementary sequences in the literature of flat-topped carbonate platforms and are commonly viewed as the result of a fully progradational phase, following a sediment starved one, during which accommodation space is passively filled (Ginsburg, 1971; Pratt & James, 1986). In this work, it is proposed that these elementary sequences may also be viewed as the result of relative sea-level changes. According to Figure 9C, the accumulation rate initially lags behind creation of accommodation space, as shown by the deposition of open subtidal facies at the base of the sequences, but progressively overtakes relative sea-level rise at highstand, filling most of the available accommodation space. The resulting deposits show a gradual shallowing-upward trend culminating in subaerial exposure. Resultant elementary sequences are thus both thickness and facies complete and can be compared to catch-up cycles (Soreghan & Dickinson, 1994; Hillgartner & Strasser, 2003). The last type of elementary sequences developed entirely in the subtidal domain (sequences 25–26 and 28–31 in Figure 3). According to Figure 9D, the sedimentation rate lags severely behind the relative sea-level rise, as shown by the deposition of more open and deeper subtidal facies of the depositional system. Subsequently, in highstand, the sedimentation rate increases resulting in a shallowing upward facies trend culminating in the deposition of strongly burrowed restricted subtidal deposits. This suggests that the sedimentation rate decreases significantly towards the top of such sequences. The deposition of more open subtidal facies is reset upon a renewed increase in accommodation space at the beginning of the next relative sea-level rise. This type of sequence compares to give-up cycles (Soreghan & Dickinson, 1994; Hillgartner & Strasser, 2003), and to subtidal cycles (sensu Osleger, 1991). Therefore, such sequences are both thickness incomplete and facies incomplete as they are the product of a carbonate factory that cannot keep up or catch up with the rising sea level.

There exists quite a good direct relationship between the thickness of elementary depositional sequences and its facies content: the thinnest sequences (from 1 to 19 in Figure 3) mostly correspond to base cutout catch-down sequences, and are characterised by a prevalence of restricted facies; the thickest ones (from 28 to 31 in Figure 3) are give-up sequences dominated by open marine facies.

Considering the thickness changes in elementary depositional sequences, as well as the variable penetration depth of vadose diagenesis, a stacking pattern of elementary sequences emerges, which suggest a hierarchy of environmental changes. Groups of three to five elementary sequences are stacked into 15 small-scale sequences (I–XV in Figure 3). Small-scale sequences I–III, VII and X are made up of only base cutout catch-down elementary sequences. Sequence boundaries are mostly placed at the top of the thinner elementary sequences showing marked evidence of subaerial exposure (elementary sequences 4, 9, 13, 15 and 18 in Figure 3). In these elementary sequences root traces and early meteoric diagenetic fabrics are distributed through almost their whole thickness. Small-scale sequences IV–VI, VIII–IX and XI–XII are made up of amalgamated elementary sequences showing a strong pedogenetic modification of primary sedimentary

features. Small-scale sequence VI corresponds to a dark horizon of black pebbles marked at the base by an erosive surface. Starting from small-scale sequence XIII, the vertical stacking pattern of elementary sequences develops more defined deepening/shallowing facies trends. Transgressive deposits are characterised by: (i) upward stacking of catch-up and give-up elementary sequences showing a facies evolution from restricted to more open-marine conditions; (ii) upward decreasing or even lacking (give-up sequences) early meteoric diagenesis and (iii) general upward-increasing thickness of elementary sequences. Conversely, regressive deposits are characterised by: (i) elementary sequences showing a facies stacking pattern evolving from open marine conditions towards more restricted ones; (ii) upward-increasing enhancement of desiccation features and (iii) general upward-decreasing thickness of elementary sequences. Consequently, the sequence boundaries of small-scale sequences XIII and XIV correspond to the top of the thinnest elementary sequences in which the meteoric overprint penetrates deeply into the underlying sequence (elementary sequences 23 and 27 for small-scale sequence XIII and XIV, respectively).

Groups of two to four small-scale sequences stack into five medium-scale sequences, four of which outcrop completely (sequences A–D in Figure 3). Medium-scale sequences A–D record only facies formed in the restricted peritidal domain showing repeated episodes of subaerial exposure. These episodes culminate with the deposition of small-scale sequences IV–VI, VIII–IX and XI–XII that, as previous discussed, are the result of the amalgamation of base cutout catch-down elementary sequences. Medium-scale sequence E is significantly thicker than A–D; moreover, it is made up of small-scale sequences recording mostly facies formed in the open marine domain (i.e. they are almost exclusively formed by catch-up and give-up elementary sequences). Transgressive deposits of medium-scale sequences are characterised by: (i) a general upward increase in the thickness of small-scale sequences (from I to II in A; from XIII to XV in medium-scale sequence E) and/or (ii) upward stacking of facies in small-scale sequences suggesting a deepening-upward trend (i.e. from facies formed mostly in restricted sub-environments to those formed in open-marine ones). However, transgressive deposits are not well represented in medium-scale sequences B–D. It is interpreted that in these medium-scale sequences, such deposits may correspond only to the thicker small-scale sequences found at their base (IV, VII and X in medium-scale B, C and D, respectively). Conversely, regressive deposits of medium-scale sequences are characterised by: (i) an upward decrease in thickness of small-scale sequences (from II to III in A; from IV to VI in B; from VII to IX in C; from X to XII in D) and/or (ii) upward stacking of facies in small-scale sequences suggesting a shallowing-upward environmental trend (i.e. from facies formed mostly in open-marine sub-environments to those formed in restricted ones). Medium-scale sequence E is not complete since it is interpreted to record only the transgressive trend.

5 | DISCUSSION

5.1 | Control processes of relative sea-level changes

In order to understand what types of processes exert a major control on the stacking pattern of shallow-water carbonate elementary sequences, both autocyclic and allocyclic mechanisms should be considered (Pratt, 2010; Strasser, 2018). Autocyclic processes are inherent to the sedimentary system and may produce 'cyclic' shallowing-up units (Ginsburg, 1971; Pratt & James, 1986). Assumptions of this model are that carbonate sedimentation stops when sediment fills the whole available accommodation space and resumes when subsidence creates water depth sufficient to start-up again the carbonate factory. In such a context, the accommodation space for the peritidal deposits is only created by constant subsidence and/or long-term sea-level rise, whereas facies distribution along the platform profile is mostly controlled by local factors as a result of unpredictable stochastic processes (Dexter et al., 2009). Autocyclic mechanisms are here excluded as the main control processes of peritidal depositional sequences for the following reasons: (i) in base cutout catch-down sequences (Figure 9B), subaerial exposure is indicated by an overprinting of subtidal facies. This is considered an unequivocal sign of allogenic forcing of the sedimentary system, since it implies a relative sea-level fall and cannot be caused by progradation or lateral migration of facies belts or changes in sediment supply (Strasser, 1991; Schlager, 2003; D'Argenio et al., 1997); (ii) the occurrence of give-up sequences implies that sedimentation was not high enough to fill the available accommodation space (Figure 9D; Osleger & Read, 1991); (iii) the hierarchical organisation in three orders of depositional sequences and the recurrence of sequence boundaries linked to different durations of subaerial exposure imply that relative sea-level changes of different amplitude and frequency played an important role in the formation of all sequences. These facies features, even if autocyclic processes cannot be excluded as contributors to the variability of the internal composition of individual sequences (Osleger, 1991; Strasser, 2018), have to be attributed to allocyclic processes either driven by tectonics or by Earth's orbital parameters (Strasser et al., 2006). Pulsation of tectonic subsidence (Cisne, 1986) may be

a valuable candidate since it theoretically could regulate the creation of accommodation space along active faults. Moreover, it was proposed that high-frequency changes in subsidence rates may produce stacking patterns of cycles like those formed under the influence of cyclical sea-level changes (Bosence et al., 2009). However, this mechanism is here excluded based on the evidence that during the Early Cretaceous the ACP was placed along the Southern Tethys Ocean passive margin in its late stage of thermal cooling, at a constant subsidence rate (Channel et al., 1979; D'Argenio & Alvarez, 1980; Ricchetti et al., 1988). Therefore, the variable depth of vadose diagenesis affecting subtidal limestones (catch-down sequences), the deposition of amalgamated brecciated sequences and the occurrence of fully subtidal (give up) sequences seems to be better explained by high-frequency eustatic sea-level changes (Figure 9). The most convincing interpretation for the described hierarchical organisation of depositional sequences is related to the Earth's orbital control. Specifically, taking into account the hierarchical stacking (bundling) of depositional sequences, it is interpreted that the maximum ratio (5:1) between elementary sequences and small-scale sequences and the maximum ratio (4:1) between small-scale sequences and medium-scale sequences may reflect the hierarchy of Milankovitch cycles as a function of the Earth's orbital parameters (Berger et al., 1989; Laskar et al., 2011). It is underlined that the occurrence of missed beats, due to low accommodation, may hinder the above-described hierarchical stacking pattern of sequences, reducing the number of elementary sequences that could form a small-scale sequence and the number of small-scale sequences that could form a medium-scale sequence (Strasser et al., 1999). Following the premises made above, it is assumed as a working hypothesis that the different types of elementary sequences may have formed in tune with the 20 kyr precession cycle. Moreover, small-scale sequences may correspond to the 100 kyr short eccentricity cycle, and medium-scale sequences to the 400 kyr long eccentricity cycle. Since the ACP was situated at approximately 20–25° of latitude during the Cretaceous (Figure 2), it is expected that the influence of the obliquity forcing was so small as to leave no clear signal that can be interpreted in terms of sea-level fluctuations. However, it is not excluded that some elementary sequences may result from a combination of precession and inclination periodicities (D'Argenio et al., 2008). This interpretation is consistent with several cyclostratigraphic studies (D'Argenio et al., 1997, 1999; Raspini 1998, 2001; Ferreri et al., 2004; Spalluto, 2008), spectral analysis of sedimentary data (Pelosi & Raspini, 1993; Longo et al., 1994; D'Argenio et al., 1999) stable isotope data (D'Argenio et al., 2004; Wissler et al., 2004; Amodio et al., 2023) and palaeomagnetic data (Iorio et al., 1996; Tarling et al., 1999) collected in several Cretaceous shallow-water carbonate successions cropping out in Southern Italy, which formed in the same palaeogeographical scenario as the ACP.

5.2 | The stacking pattern of peritidal sequences: a sequence stratigraphic perspective

Following the premises shown in Section 5.1, based on the conceptual model shown in Figure 9, and on the time frame given by the cyclostratigraphic interpretation, the evolution through time of the relative sea-level curve has been plotted in Figure 10. The time steps are given by the 20 kyr interval attributed to the formation of each elementary sequence. Furthermore, it is assumed that the sea-level fluctuations were symmetrical under greenhouse conditions where insolation changes are more or less directly translated into sea-level changes (Read et al., 1995). Where one 100 kyr sequence contains less than five elementary sequences, it is assumed that the missing ones were not recorded due to low accommodation at a small-scale sequence boundary. Similarly, where one 400 kyr sequence contains less than four small-scale sequences, it is assumed that the missing ones were not recorded due to low accommodation at a medium-scale sequence boundary. The dotted relative sea-level curve drawn in the three brecciated layers is purely interpretive since elementary sequences are not recorded due to amalgamation and condensation following prolonged subaerial exposure. As shown in Figure 9, even if some elementary sequences are recorded during this interval they were completely brecciated by subsequent subaerial exposure. According to Goldhammer et al. (1990), these condensed intervals are those more prone to record 'missed beats'.

Given the time frame based on cyclostratigraphy shown in Figure 10, it is suggested that much of the time necessary to form the studied succession (about 1.2 Myr, i.e. the sum of time needed to form the B, C and D medium-scale sequences) is spent in the formation of the approximately 3 m thick interval mostly made up of amalgamated elementary sequences. This latter interval, which follows the deposition of the first interval, is about 2.9 m thick, entirely formed by base cutout elementary sequences, whose stacking-pattern builds the small-scale sequences I, II and III of the medium-scale sequence A (Figure 10A). Conversely, the thicker middle and upper parts of the succession were formed in a significantly shorter time interval (about 280 kyr) than the thinner lower part. In more detail, it emerges that the middle part is mostly formed by catch-up sequences and, subordinately, by give-up sequences, building small-scale sequences XIII and XIV of the medium-scale sequence E (Figure 10B,C); while, the

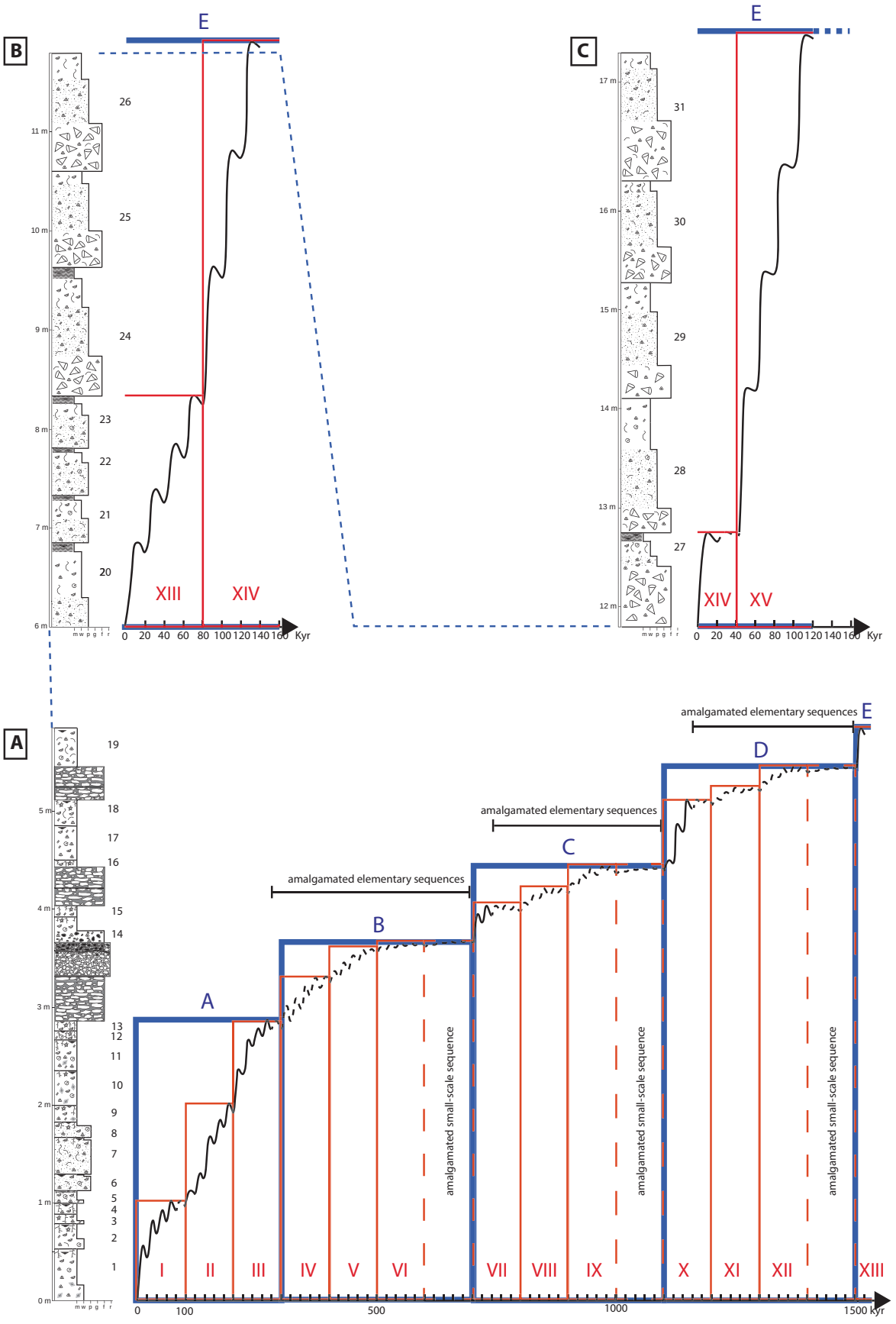

FIGURE 10 Relative sea-level curve reconstructed respectively for the lower (A), middle (B) and upper part (C) of the studied succession. For facies explanation, elementary, small-scale and medium-scale sequences interpretation see legend to Figure 3 and text. For the interpretation of sea-level amplitude of each elementary sequence see the model shown in Figure 9.

upper part is entirely made up of give-up sequences building the small-scale sequence XV (not completely outcropping) of medium-scale sequence E (Figure 10C).

Consequently, it is inferred that the lower part of the studied succession, corresponding to approximately one-third of the total thickness, was deposited in about 1.5 Myr, a time span covering over 80% of the time needed to form the whole succession. In contrast, the middle and upper parts of the studied succession, corresponding to approximately two-third of the total thickness, were deposited in about 280 kyr, a time span that covers less than 20% of the time needed to form the whole succession. This apparent discrepancy may be easily explained by looking at Figure 10. The first part of the succession consists exclusively of base cutout catch-down sequences and by amalgamated ones. This indicates that most of the time was spent in subaerial exposure rather than carbonate sedimentation. During this time interval, the accommodation potential (i.e. the space available for potential sediment accumulation—Jervey, 1988) on the platform was becoming increasingly limited, allowing the deposition of thin elementary sequences prone to early meteoric vadose diagenesis (catch-down sequences), evolving upward to amalgamated sequences. In contrast, the middle and the upper parts are made up of thicker catch-up and give-up sequences. This indicates that a significant portion of the time needed to form these sequences was spent in carbonate sedimentation during a time interval in which the accommodation potential was becoming increasingly high, allowing the deposition of catch-up elementary sequences evolving upward to fully subtidal give-up sequences.

If relative sea-level changes control changes in accommodation space, sequence-stratigraphic concepts can be applied to interpret the stacking pattern of aggrading peritidal sequences (Goldhammer et al., 1990; Strasser, 1994; Strasser et al., 1999; Raspini, 2001; D'Argenio et al., 2008), even though the application of this methodology in these settings presents some limitations. First of all, typical geometries of marginal marine sequences (such as onlap, downlap, offlap, toplap stratal relationships) do not develop in peritidal settings, where systems tracts have an aggradational architecture. Furthermore, peritidal successions are punctuated by several discontinuities due to periodic exposures, which may result in erosion or non-deposition of some sequences (Goldhammer et al., 1990). Consequently, identification of complete sequences and systems tracts often is not possible. Nonetheless, long-term transgressive and regressive facies trends can be identified in the stacking pattern of high-frequency sequences that formed in time intervals corresponding to the duration of third-order depositional sequences (Montañez & Osleger, 1993; D'Argenio et al., 1997, 1999, 2004, 2008; Strasser et al., 2000). According to Montañez and Osleger (1993), sequence boundaries and transitions between systems tracts on flat-topped platform may develop as zones rather than distinct horizons because of the effect of the higher-frequency sea-level signal superimposed on the long-term, third-order trend. Consequently, sequence boundary and maximum-flooding zones are individuated, and between these zones transgressive and regressive deposits, respectively, are recognised. Moreover, according to Strasser et al. (2000), the cyclostratigraphic interpretation of peritidal succession reveals that third-order sequences may have formed in tune with the 400 kyr eccentricity cycle of Earth's orbit or multiples thereof.

The long-term relative sea-level curve in the studied succession is obtained by plotting the envelope of high-frequency relative sea-level changes (Figure 11). The slope of this curve varies along the succession and reflects changes in accommodation space over time. Specifically, if the slope of the curve decreases there is a progressive loss of accommodation space on the platform, until reaching zero accommodation when the curve flattens. The lower part of the succession shows exactly this type of evolution. The first interval, corresponding to the outcropping thickness of the medium-scale sequence A, consists of three distinct small-scale sequences completely made up of base cutout catch-down sequences. According to the interpretation shown in Figure 11, it was formed over about 300 kyr and is built by regressive peritidal deposits that accumulate at the end of the third-order highstand (late highstand deposits) when accommodation space progressively shrinks and, consequently, small-scale sequences become thinner and thinner. At the same time, small-scale sequence boundaries are well-marked subaerial exposure surfaces showing increasing evidence of early meteoric vadose features (Figures 3, 6 and 10A). The second interval lasts close to 400 kyr and corresponds to the medium-scale sequence B. It is completely made up of condensed elementary sequences forming the first of the three brecciated intervals (Figures 3, 4, 6 and 10A). This interval is bounded by a well-cemented palaeosol rich in black pebbles that is interpreted as the most prominent evidence of prolonged subaerial exposure (>100 kyr long in Figures 10A and 11) in the whole succession (Figure 6). Following the definition of Montañez and Osleger (1993), it can be interpreted as a sequence-boundary zone since it was formed in a period of significant loss of accommodation. These deposits may also be described as the result of the forced regression imposed by the high-frequency signal that is superimposed on the third-order one (i.e. the falling stage systems tract sensu Plint and Nummedal, 2000; Coe et al., 2003). Therefore, in Figure 11 it is proposed to call this interval as a sequence-boundary zone or falling-stage deposit. In this context, even if some elementary

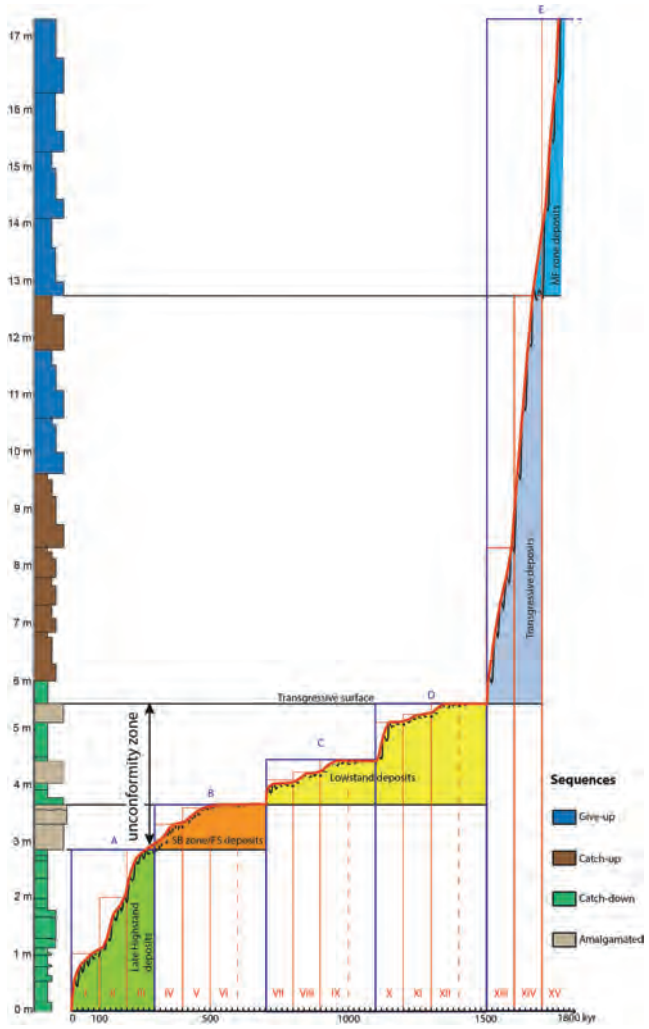

FIGURE 11 Long-term relative sea-level curve plotted against different types of elementary sequences. FS, falling stage; SB: sequence boundary. For more explanation, refer to the text.

sequences were formed during high-frequency sea-level rises, they were completely brecciated during subsequent prolonged subaerial exposure (see Figure 9A) until reaching the condition of zero accommodation (Figure 11). Above this interval the other two breccia layers occur separated from each other by a few base cutout catch-up sequences (Figures 3, 10A and 11). This interval lasts about 800 kyr, corresponding to the cumulative duration of medium-scale sequences C and D and is here interpreted as formed by lowstand deposits (Figure 11). They represent the sedimentary accumulation that straddles the lowest position of the relative sea-level curve. Moreover, in contrast to the underlying interval, a small recovery of accommodation space is recorded by the preservation of a few elementary sequences (14–15 and 16–18 in Figures 3 and 10A) that formed during medium-scale transgression. After the deposition of the last of the three brecciated layers, the subsequent stacking pattern of elementary sequence sets supports a rapid recovery of the accommodation space on the platform marked by the rapidly increased slope inclination of the long-term curve (Figure 11). This interval lasted about 200 kyr and is made up of catch-up sequences that become gradually thicker upward, passing to fully subtidal give-up sequences (see sequences 19–27 in Figures 3 and 10A,B,C). This interval is thus interpreted as made by transgressive deposits accumulated from the onset of the transgression until the time of maximum transgression. This latter is interpreted to correspond to the stacking pattern of the thicker give-up sequences forming an about 4 m thick interval at the top of the succession (see sequences 28–31 in Figures 3 and 10C). This interval, lasting about 80 kyr, is here interpreted to correspond to the maximum-flooding zone.

5.3 | Sequence chronostratigraphy

Although the chronostratigraphic resolution of the studied peritidal carbonates is not very precise as biostratigraphic data are based only on the stratigraphic distribution of benthic foraminifers (Spalluto & Caffau, 2010), a tentative correlation was already proposed by Spalluto (2012) between the peritidal succession cropping out in the northern Murge area and the main long-term transgressive/regressive cycles published in the sequence-chronostratigraphic chart for European basins (Hardenbol et al., 1998). The sequence boundary zone also described in the present study was correlated with the Al 7 sequence boundary (102.12 Myr) of the chronostratigraphic chart, which marks the transition between the middle and late Albian (Spalluto, 2012). This correlation was supported by the last occurrence of early Albian taxa in late highstand deposits of the studied succession and by the first occurrence of late Albian primitive orbitolinid assemblages in transgressive deposits above the sequence boundary zone (see Section 4.2). According to Hardenbol et al. (1998), this sequence boundary, recognised both in Tethys and Boreal domains, marks the boundary between the *Euhoplites lautus* ammonite zone and the *Dipoloceras cristatum* Ammonite Subzone in southern Europe. This sequence boundary is also shown in the revised eustatic curve of the Cretaceous (Haq, 2014) and corresponds to KAl4 (107.5 Myr; Figure 12). Comparing the expected duration of the studied succession, based on cyclostratigraphic and sequence stratigraphic interpretation (Figures 10 and 11), with the one shown in the eustatic curve (red curve in Figure 12), seems to suggest a match. Specifically, the interval of time delimited by the segment of the eustatic curve between the late highstand of the sequence below the Kl4 boundary and the

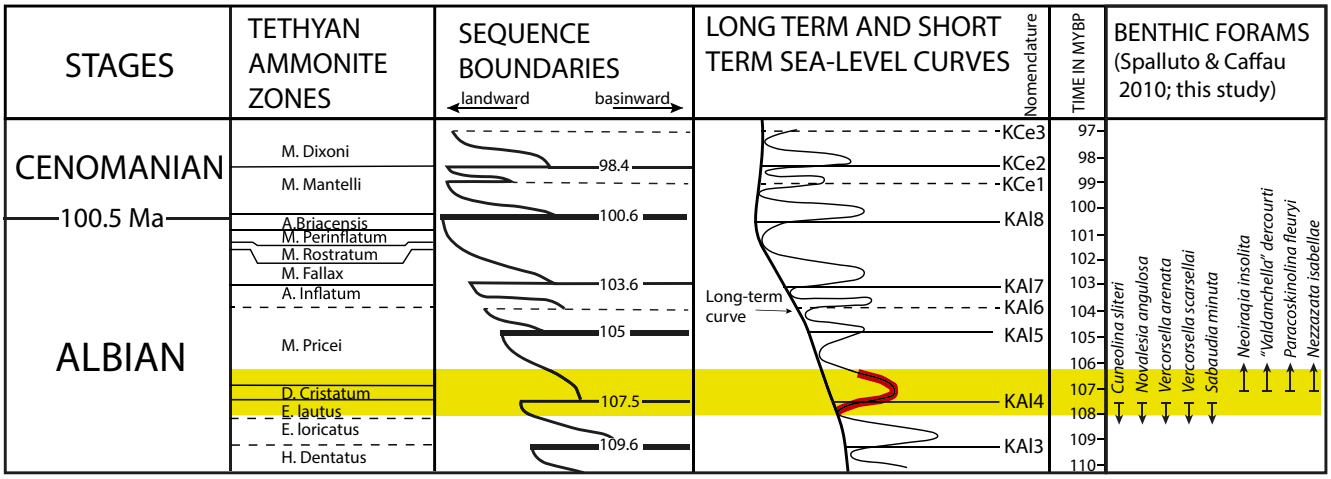

FIGURE 12 Cretaceous Eustatic Cycle Chart simplified and redrawn from Haq (2014). Note that the short-term sea-level curve in Haq (2014) corresponds to the third-order one. In the yellow rectangle the time span covered by the studied succession. Note that the red highlighted line of the short-term sea-level curve may correspond to the third-order sea-level curve drawn in Figure 11.

maximum drowning of the sequence above is more than 1.5 Myr, approaching the 1.8 Myr supposed in this paper. Although this evidence cannot be considered conclusive, pending the possibility of proposing a better chronostratigraphic resolution of the studied succession, the working hypothesis based on Milankovitch cycles may be still considered reliable.

6 | CONCLUSIONS

The studied peritidal succession is a small piece of an impressive 6–7 km thick aggrading Mesozoic succession formed in low-energy muddy tidal flats and lagoons developed in the interior part of the ACP. It reveals how Cretaceous peritidal carbonates, developed along the mature passive margin of southern Tethys Ocean, may have responded to sea-level oscillations of different amplitude under greenhouse conditions.

This study, based on centimetre-scale facies details, allows the following conclusions to be highlighted:

(i) Six main facies, formed in the low-energy internal sector of the ACP, have been identified. Periods of prolonged exposure were revealed by the deposition of three layers of brecciated palaeosols, the presence of which in the lower part of the studied succession testifies to an important interruption in shallow marine carbonate sedimentation.

(ii) The hierarchical stacking pattern of sequences in beds and bedsets reveals a Milankovitch cyclicity, even if the low chronostratigraphic resolution, based only on benthic foraminifer biostratigraphy, does not allow this hypothesis to be fully supported. Elementary sequences are assumed to represent the precession cycle (*ca* 20 kyr), and small and medium-scale sequences the short (*ca* 100 kyr) and long (*ca* 400 kyr) eccentricity cycles, respectively.

(iii) The basic building blocks of the studied succession are made up of four different types of elementary sequences (condensed, catch-down, catch-up and give up), which show specific facies organisations. Furthermore, the different types of elementary sequences are not randomly distributed in the succession, but occur repetitively in specific stratigraphic intervals. Based on the facies interpretation, elementary sequences are interpreted in terms of relative sea-level changes, and subsequently, the relative sea-level curve of the entire succession was reconstructed using a time step of 20 kyr (i.e. the duration of the precession cycle), in order to show how the accommodation space changed over time.

(iv) The envelope of the reconstructed relative sea-level curve was used to represent the long-term (third order) accommodation change on the platform and is interpreted with a sequence stratigraphic perspective. It emerges that the studied succession, 17 m thick, was formed over approximately 1.8 Myr. Most of this time was spent in subaerial exposure, as approximately 1.2 Myr was predicted to be condensed in a stratigraphic interval less than 3 m thick. This interval encompasses both the sequence boundary zone/falling stage deposits and the lowstand deposits of the sequence lying above the late highstand deposits, these latter formed over about 300 kyr. The subsequent transgressive deposits consist mostly of catch-up elementary sequences that pass upward to give-up elementary

sequences. These latter are interpreted to represent the maximum-flooding deposits. This transgressive interval corresponds to about two-third of the total thickness of the studied succession and was formed in only 280 kyr.

(v) One of the main implications of this study is that in peritidal successions the main unconformities do not necessarily correspond to single surfaces but, rather, to very condensed intervals or 'unconformity zones' (i.e. the sum of sequence boundary zone/falling stage deposits and lowstand deposits). It is worth noting that the reduced thickness of the unconformity zones cannot be resolved at seismic-scale resolution, where they can be interpreted as single surface sequence boundaries. Furthermore, peritidal successions are mostly built during long-term transgressions, when the rapid gain of accommodation space on the platform (i.e. the sum of subsidence and long-term sea-level rise) creates the optimal condition for the preservation of most of high-frequency 'beats'.

(vi) Based on published biostratigraphic data, the large-scale sequence boundary zone of this study is correlated with the third-order KAl4 sequence boundary of the Cretaceous eustatic cycle chart. This correlation opens an interesting scenario to compare the impact of eustatic sea-level changes in coeval stratigraphic successions formed worldwide in different palaeogeographical settings.

ACKNOWLEDGEMENTS

We are very grateful to our mentor Piero Pieri who introduced us to carbonate sedimentology. André Strasser and an anonymous reviewer are thanked for the many suggestions and comments that allowed us to improve our manuscript. The Editor-in-Chief, Peter Swart, and Associate Editor, Valentina Rossi, are thanked for their excellent editorial work. Research activities discussed in this paper have benefited from the following funds: PRIN Project 2022 "Abrupt Lithofacies Variations IN the stratigraphic record: proxies for environmental and climate changes - ALVIN" (P.I. S. Cirilli, local A.I M. Tropeano) Grant/Award number 2022APF9M2; Carg Project (ISPRA) for the geological mapping of the 438 Sheet Bari grant to Luisa Sabato; Phd funds of Bari University awarded to Marco Petruzzelli.

CONFLICT OF INTEREST STATEMENT

The authors have no conflicts of interest to declare.

DATA AVAILABILITY STATEMENT

Data available on request from the authors.

ORCID

Luigi Spalluto https://orcid.org/0000-0001-9439-6461

REFERENCES

Amodio, S., Barattolo, F. & Parente, M. (2023) The early cretaceous C-isotope record of shallow-marine carbonates: A transect across southern Alps, Apennines and Dinarides. *Rendiconti online Società Geologica Italiana*, 59, 28–34.

Antonelli, M., Petti, F.M., Conti, J., Sacco, E., Petruzzelli, M., Spalluto, L. & Wagensommer, A. (2023) Lower Cretaceous dinosaur footprints from the Molfetta tracksite (Apulia, southern Italy). *Cretaceous Research*, 142, 105388.

Arnaud Vanneau, A. & Sliter, W. (1995) Early cretaceous shallow-water benthic foraminifers and fecal pellets from leg 143 compared with coeval faunas from the Pacific Basin, Centeral America, and the Tethys. *Proceedings of the Ocean Drilling Program, Scientific Results*, 143, 537–564.

Assereto, R.L. & Kendall, C.G.S.C. (1977) Nature, origin and classification of peritidal tepee structures and related breccias. *Sedimentology*, 24, 153–210.

Azeredo, A.C., Wright, V.P., Mendonca-Filho, J., Cabral, M.C. & Duarte, L.V. (2015) Deciphering the history of hydrologic and climatic changes on carbonate lowstand surfaces: calcrete and organic-matter/evaporite facies association on a palimpsest Middle Jurassic landscape from Portugal. *Sedimentary Geology*, 323, 66–91.

Berger, A., Loutre, V. & Dehant, V. (1989) Astronomical frequencies for pre-Quaternary palaeoclimate studies. *Terra Nova*, 5, 474–479.

Berkeley, A. & Rankey, E.C. (2012) Progradational Holocene carbonate tidal flats of Crooked Island, south-east Bahamas: an alternative to the humid channelled belt model. *Sedimentology*, 59, 1902–1925.

Bosellini, A. (2002) Dinosaurs re-wright the geodynamics of the eastern Mediterranean and the paleogreography of the Apulian Platform. *Earth Science Reviews*, 59, 211–234.

Bosence, D., Procter, E., Aurell, M., Bel Kahla, A., Boudagher-Fadel, M., Casaglia, F., Cirilli, S., Mehdie, M., Nieto, L., Rey, J., Scherreiks, R., Soussi, M. & Waltham, D. (2009) A dominant tectonic signal in high-frequency, peritidal carbonate cycles? A regional analysis of Liassic platforms from western Tethys. *Journal of Sedimentary Research*, 79, 389–415.

Carannante, G., Ruberti, D. & Sirna, M. (2000) Upper Cretaceous ramp limestones from the Sorrento Peninsula (southern Apennines, Italy): micro- and macrofossil associations and their significance in the depositional sequences. *Sedimentary Geology*, 132, 89–123.

Channel, J.E.T., D'Argenio, B. & Horvath, F. (1979) Adria, the African Promontory, in Mesozoic Mediterranean palaeogeography. *Earth Science Reviews*, 15, 213–292.

Ciaranfi, N., Pieri, P. & Ricchetti, G. (1988) Note alla carta geologica delle Murge e del Salento (Puglia centromeridionale). *Memorie della Societa Geologica Italiana*, 41, 449–460.

Cisne, J.L. (1986) Earthquakes recorded stratigraphically on carbonate platforms. *Nature*, 323, 320–322.

Coe, A., Bosence, D., Church, K., Flint, S., Howell, J. & Wilson, R. (2003) *The sedimentary record of sea-level change*. Cambridge: The Open University.

Crescenti, U. & Vighi, L. (1964) Caratteristiche, genesi e stratigrafia dei depositi bauxitici del Gargano e delle Murge; cenni sulle argille con pisoliti bauxitiche del Salento (Puglia). *Bollettino della Societa Geologica Italiana*, 83, 5–51.

D'Argenio, B. (1974) Le piattaforme carbonatiche periadriatiche. Una rassegna di problemi nel quadro geodinamico mesozoico dell'area mediterranea. *Memorie della Societa Geologica Italiana*, 13, 137–160.

D'Argenio, B. & Alvarez, W. (1980) Stratigraphic evidence for crustal thickness changes on the southern Thetyan margin during the Alpine cycle. *Geological Society of America Bulletin*, 91, 681–689.

D'Argenio, B., Ferreri, V. & Amodio, S. (2008) Sequence stratigraphy of Cretaceous carbonate platforms: a cyclostratigraphic approach. *Geoacta, Special Publication*, 1, 157–171.

D'Argenio, B., Ferreri, V., Amodio, S. & Pelosi, N. (1997) Hierarchy of high-frequency orbital cycles in Cretaceous carbonate platform strata. *Sedimentary Geology*, 113, 169–193.

D'Argenio, B., Ferreri, V., Raspini, A., Amodio, S. & Buonocunto, F.P. (1999) Cyclostratigraphy of a carbonate platform as a tool for high-precision correlation. *Tectonophysics*, 315, 357–385.

D'Argenio, B., Ferreri, V., Weissert, H., Amodio, S., Buonocunto, F.P. & Wissler, L. (2004) A multidisciplinary approach to global correlation and Geochronology. The Cretaceous shallow-water carbonates of southern Apennines, Italy. In: D'Argenio, B., Fischer, A.G., Premoli Silva, I., Weissert, H. & Ferreri, V. (Eds.) *Cyclostratigraphy: approaches and case histories*, Vol. 81. Tulsa, Oklahoma, USA: SEPM, Special Publication, pp. 103–122.

Demicco, R.V. & Hardie, L.A. (1994) *Sedimentary structures and early diagenetic features of shallow marine carbonate deposits*. Tulsa, Oklahoma, USA: SEPM, Atlas Series Number 1.

Dexter, T.A., Kowalewski, M. & Read, J.F. (2009) Distinguishing Milankovitch-driven processes in the rock record from stochasticity using computer-simulated stratigraphy. *Journal of Geology*, 117, 349–361.

Dunham, R.J. (1969) *Vadose compaction on Cayo Arenas, Campeche Banks*, 1. AAPG Memoir, 108-121.

Dunham, R.K. (1962) Early vadose silt in Townsend mound (reef), New Mexico. In: Friedman, G.M. (Ed.) *Depositional environments in carbonate rocks*, Vol. 14. Tulsa, Oklahoma, USA: SEPM, Special Publication, pp. 139–181.

Eberli, G.P. (2013) The uncertainties involved in extracting amplitude and frequency of orbitally driven sea-level fluctuations from shallow-water carbonate cycles. *Sedimentology*, 60, 64–84.

Eberli, G.P., Anselmetti, F.S., Betzler, C., Van Konijnenburg, J.-H. & Bernoulli, D. (2004) Carbonate platform to basin transitions on seismic data and in outcrops: Great Bahama Bank and the Maiella Platform margin, Italy. In: *Seismic imaging of carbonate reservoirs and systems*, Vol. 81. AAPG Memoir, pp. 207–250.

Embry, A.F. & Klovan, J.E. (1971) A Late Devonian reef tract on northeastern Banks Island, N.W.T. *Bulletin of Canadian Petroleum Geology*, 19, 730–781.

Enos, P. (1983) Shelf. In: Scholle, P.A., Bebout, D.G. & Moore, C. (Eds.) *Carbonate depositional environments*, Vol. 33. Tulsa, Oklahoma, USA: AAPG Memoir, pp. 268–295.

Esteban, M. & Klappa, C.F. (1983) Subaerial exposure environment. In: Scholle, P.A., Bebout, D.G. & Moore, C. (Eds.) *Carbonate depositional environments*, Vol. 33. Tulsa, Oklahoma, USA: AAPG Memoir, pp. 1–54.

Ferreri, V., Amodio, S., Sandulli, R. & D'Argenio, B. (2004) Orbital chronostratigraphy of the Valanginian-Hauterivian boundary: a cyclostratigraphic approach. In: D'Argenio, B., Fischer, A.G., Premoli, S.I., Weissert, H. & Ferreri, V. (Eds.) *Cyclostratigraphy: approaches and case histories*, Vol. 81. Tulsa, Oklahoma, USA: SEPM, Special Publication, pp. 153–166.

Flügel, E. (2004) *Microfacies of carbonate rock: analysis, interpretation and application*. Berlin: Springer-Verlag.

Gallo Maresca, M. (1994) Aspetti tassonomici e biostratigrafici delle Radiolitdae albiane delle Murge e del Gargano (Puglia, Italia meridionale). *Palaeopelagos*, 4, 223–232.

Ginsburg, R.N. (1971) Landward movement of carbonate mud: new model for regressive cycles in carbonates (abstract). *Bulletin American Association Petroleum Geology*, 55, 340.

Goldhammer, R.K., Dunn, P.A. & Hardie, L.A. (1990) Depositional cycles, composite sea-level changes, cycle stacking patterns, and the hierarchy of stratigraphic forcing: examples from Alpine Triassic platform carbonates. *Geological Society of America Bulletin*, 102, 535–562.

Graziano, R. (2013) Sedimentology, biostratigraphy and event stratigraphy of the Early Aptian oceanic anoxic event (OAE1A) in the Apulia Carbonate Platform margin—Ionian basin system (Gargano Promontory, southern Italy). *Cretaceous Research*, 39, 78–111.

Graziano, R., Raspini, A. & Spalluto, L. (2013) High-resolution ^{13}C stratigraphy through the Selli Oceanic Anoxic Event (OAE1a) in the Apulia Carbonate Platform: the Borgo Celano section (western Gargano Promontory, Southern Italy). *Italian Journal of Geosciences*, 132(3), 477–496.

Haq, B.U. (2014) Cretaceous eustasy revisited. *Global and Planetary Change*, 113, 44–58.

Hardenbol, J., Thierry, J., Farley, M.B., Jacquin, T., De Graciansky, P.C. & Vail, P.R. (1998) Mesozoic and Cenozoic sequence chronostratigraphic framework of European basins. In: De Graciansky, P.C., Hardenbol, J., Jacquin, T. & Vail, P.R. (Eds.) *Mesozoic and Cenozoic sequence stratigraphy of European basins*, Vol. 60. Tulsa, Oklahoma, USA: SEPM Special Publication.

Hardie, L.A. (1977) *Sedimentation on modern carbonate tidal flats of northwest Andros Island, Bahamas*. Baltimore, Maryland, USA: John Hopkins University Press.

Hardie, L.A. & Shinn, E.A. (1986) Carbonate depositional environments, modern and ancient part 3: Tidal flats. *Colorado School of Mines Quarterly*, 81, 1–74.

Hillgartner, H. & Strasser, A. (2003) Quantification of high-frequency sea-level fluctuations in shallow-water carbonates: an example from the Berriasian-Valanginian (French Jura). *Palaeogeography Palaeoclimatology Palaeoecology*, 200, 43–63.

Husinec, A. & Sokać, B. (2006) Early Cretaceous benthic associations (foraminifera and calcareous algae) of a shallow tropical-water platform environment (Mljet Island, southern Croatia). *Cretaceous Research*, 27, 418–441.

Iorio, M., Tarling, D.H., D'Argenio, B. & Nardi, G. (1996) Ultra-fine magnetostratigraphy of Cretaceous shallow water carbonates, Monte Raggeto, southern Italy. In: Morris, A. & Tarling, D.H. (Eds.), *Paleomagnetism and tectonics of the Mediterranean region*, Vol. 105. London: Geological Society of London, Spec. Publ., pp. 195–203.

Jervey, M.T. (1988) Quantitative geological modeling of siliciclastic rock sequences and their seismic expression. In: Wilgus, C.K., Hasting, B.S., Kendall, C.G.S.C., Posamentier, H.W., Ross, C.A. & Van Wagoner, J.C. (Eds.) *Sea-level changes: an integrated approach*, Vol. 42. Tulsa, Oklahoma, USA: SEPM, Special Publication, pp. 47–69.

Jones, B. & Desrochers, A. (1992) Shallow platform carbonates. In: Walker, R.G. & James, N.P. (Eds.) *Facies models: response to sea level change*. Ottawa, Canada: Geological Association of Canada, pp. 277–301.

Kemp, D.B. & Sadler, P.M. (2014) Climatic and eustatic signals in a global compilation of shallow marine carbonate accumulation rates. *Sedimentology*, 61, 1286–1297.

Laskar, J., Fienga, A., Gastineau, M. & Manche, H. (2011) La2010: A new orbital solution for the long-term motion of Earth. *Astronomy Astrophysics*, 532(A89), 1–15.

Le Goff, J., Cerepi, A., Ghysels, G., Swennen, R., Loisy, C., Heba, G., El Desouky, H. & Muskaä, K. (2015) Meter-scale cycles as a proxy for the evolution of the Apulian Carbonate Platform during the late Cretaceous (Llogara Pass, Albania). *Facies*, 61, 21.

Logan, B.W., Rezak, R. & Ginsburg, R.N. (1964) Classification and environmental significance of algal stromatolites. *Journal of Geology*, 72, 517–533.

Longo, G., D'Argenio, B., Ferreri, V. & Iorio, M. (1994) Fourier evidence for high frequency astronomical cycles recorder in Early Cretaceous carbonate platform strata, Monte Maggiore southern Apennines, Italy. In: De Boer, P.L. & Smith, D.G. (Eds.) *Orbital forcing and cyclic sequences*, Vol. 19. Oxford, UK: IAS Special Publication, pp. 77–85.

Luperto Sinni, E. (1996) Sintesi delle conoscenze biostratigrafiche del Cretaceo del Gargano e delle Murge. *Memorie della Societa Geologica Italiana*, 51, 995–1018.

Luperto Sinni, E. & Borgomano, J. (1994) Stratigrafia del Cretaceo superiore in facies di scarpata di monte sant'Angelo (promontorio del Gargano). *Bollettino Società Geologica Italiana*, 113, 355–382.

Martin-Chivelet, J. & Gimenez, R. (1992) Paleosols in microtidal sequences: Sierra de Utiel Formation, Upper Cretaceous, SE Spain. *Sedimentary Geology*, 81, 125–145.

Montañez, I.A. & Osleger, D.A. (1993) Parasequence stacking patterns, third-order accommodation events, and sequence stratigraphy of Middle to Upper Cambrian platform carbonates, Bonanza King Formation, southern Great Basin. *AAPG Memoir*, 57, 305–326.

Nicolai, C. & Gambini, R. (2008) Structural architecture of the Adria platform-to-basin transition. *Bollettino della Società Geologica Italiana, Special Issue*, 7, 21–37.

Osleger, D. (1991) Subtidal carbonate cycles: implications for allocyclic vs. autocyclic controls. *Geology*, 19, 917–920.

Osleger, D. & Read, J.F. (1991) Relation of eustasy to stacking patterns of meter-scale carbonate cycles, Late Cambrian. USA. *Journal of Sedimentary Petrology*, 61, 1225–1252.

Patacca, E. & Scandone, P. (2013) Il Contributo degli studi stratigrafici di superficie e sottosuolo alla conoscenza dell'Appennino Lucano. Proceedings of the Atti del Congresso Ricerca, Sviluppo e Utilizzo delle Fonti Fossili: Il Ruolo del Geologo, Potenza, Italy, 30 November–2 December 2013; 97–153.

Pelosi, N. & Raspini, A. (1993) Analisi spettrale della ciclicità di alta frequenza in successioni carbonatiche neritiche di limitato spessore. Il caso del Cretacico dei Monti di Sarno (Campania). *Giornale di Geologia*, 55(1), 37–49.

Petti, F.M., Petruzzelli, M., Conti, J., Spalluto, L., Wagensommer, A., Lamendola, M., Francioso, R., Montrone, G., Sabato, L. & Tropeano, M. (2018) The use of aerial and close-range photogrammetry in the study of dinosaur tracksites: lower Cretaceous (upper Aptian/lower Albian) Molfetta ichnosite (Apulia, southern Italy). *Palaeontologia Electronica*, 21(3), 1–19.

Petti, F.M., Antonelli, M., Sacco, E., Conti, J., Petruzzelli, M., Spalluto, L., Cardia, S., Festa, V., La Perna, R., Marino, M., Marsico, A., Sabato, L., Tropeano, M., Barracane, G., Montrone, G., Piscitelli, A. & Francescangeli, R. (2022) Geothematic map of the Altamura dinosaur tracksite (early Campanian, Apulia, southern Italy). *Geological Field Trips and Maps*, 14(1.1), 1–19.

Plint, A.G. & Nummedal, D. (2000) The falling stage systems tract: recognition and importance in sequence stratigraphic analysis. In: Hunt, D. & Gawthorpe, R.L. (Eds.) *Sedimentary response to forced regression*, Vol. 172. London, UK: Geological Society London, Special Publication, pp. 1–17.

Pratt, B.R. (2010) Peritidal carbonates. In: James, N.P. & Dalrymple, W. (Eds.), Vol. 4. Facies models, pp. 401–420.

Pratt, B.R. & James, N.P. (1986) The St George Group (Lower Ordovician) of western Newfoundland: tidal flat Island model for carbonate sedimentation in shallow epeiric seas. *Sedimentology*, 33, 313–343.

Raspini, A. (1998) Microfacies analysis of shallow water carbonates and evidente of hierarchically organized cycles: Aptian of Monte Tobenna, southern Apennines, Italy. *Cretaceous Research*, 19, 197–223.

Raspini, A. (2001) Stacking pattern of cyclic carbonate platform strata: lower Cretaceous of southern Apennines, Italy. *Journal of the Geological Society of London*, 158, 353–366.

Read, J.F., Kerans, C., Weber, L.J., Sarg, J.F. & Wright, F.M. (1995) *Milankovitch sea-level changes, cycles, and reservoirs on carbonate platforms in greenhouse and icehouse worlds*. Tulsa, Oklahoma, USA: SEPM. Short Course 35.

Ricchetti, G. (1975) Nuovi dati stratigrafici sul Cretaceo delle Murge emersi da indagini nel sottosuolo. *Bollettino della Societa Geologica Italiana*, 94(3), 1013–1108.

Ricchetti, G., Ciaranfi, N., Luperto Sinni, E., Mongelli, F. & Pieri, P. (1988) Geodinamica ed evoluzione sedimentaria e tettonica dell'avampaese apulo. *Memorie della Societa Geologica Italiana*, 41, 57–82.

Schlager, W. (2003) Accommodation and supply—a dual control on stratigraphic sequences. *Sedimentary Geology*, 86, 111–136.

Schlager, W. (2005) *Carbonate sedimentology and sequence stratigraphy*. Tulsa, Oklahoma, USA: SEPM, Concepts in Sedimentology and Paleontology.

Selli, R. (1962) Il Paleogene nel quadro della geologia dell'Italia meridionale. *Memorie della Societa Geologica Italiana*, 3, 737–789.

Shinn, E.A. (1968) Practical significance of birdseye structures in carbonate rocks. *Journal of Sedimentary Petrology*, 38, 215–223.

Shinn, E.A. (1983) Tidal flat environment. In: Scholle, P.A., Bebout, D.G. & Moore, C. (Eds.) *Carbonate depositional environments*, Vol. 33. Tulsa, Oklahoma, USA: AAPG Memoir, pp. 171–210.

Shinn, E.A., Lloyd, R.M. & Ginsburg, R.N. (1969) Anatomy of a modern carbonate tidal flat, Andros Island, Bahamas. *Journal of Sedimentary Petrology*, 39, 1202–1228.

Simone, L., Carannante, G., Ruberti, D., Sirna, M., Sirna, G., Laviano, A. & Tropeano, M. (2003) Rudist-rich bodies development and growth in central southern Italy early Senonian carbonate shelves: high-energy vs low-energy settings. *Palaeogeography Palaeoclimatology Palaeoecology*, 200, 5–29.

Soreghan, G.S. & Dickinson, W.R. (1994) Generic types of stratigraphic cycles controlled by eustasy. *Geology*, 22(8), 759–761.

Spalluto, L. (2008) Sedimentology and high-resolution sequence stratigraphy of a Lower Cretaceous shallow-water carbonate succession from the western Gargano Promontory (Apulia, southern Italy). *Geoacta, Special Publication*, 1, 173–192.

Spalluto, L. (2012) Facies evolution and sequence chronostratigraphy of a "mid"-Cretaceous shallow-water carbonate succession of the Apulia Carbonate Platform from the northern Murge area (Apulia, southern Italy). *Facies*, 58, 17–36.

Spalluto, L. & Caffau, M. (2010) Stratigraphy of the mid-Cretaceous shallow-water limestones of the Apulia Carbonate Platform (Murge, Apulia, southern Italy). *Italian Journal of Geosciences*, 129, 335–352.

Spalluto, L., Caffau, M. & De Giorgio, G. (2008) The upper Albian-lower Cenomanian inner shelf carbonate succession of the Calcare di Bari Fm. from the Murge area (Apulia, southern Italy). *Rendiconti Online della Società Geologica Italiana*, 2, 181–186.

Spalluto, L. & Pieri, P. (2008) Carta geologica delle unità carbonatiche mesozoiche e cenozoiche del Gargano sud-occidentale: nuovi vincoli stratigrafici per l'evoluzione tettonica dell'area. *Memorie Descrittive della Carta Geologica d'Italia*, 78, 147–176.

Spalluto, L., Pieri, P. & Ricchetti, G. (2005) Le facies carbonatiche di piattaforma interna del Promontorio del Gargano: implicazioni paleoambientali e correlazioni con la coeva successione delle Murge. (Italia meridionale, Puglia). *Bollettino della Societa Geologica Italiana*, 124, 675–690.

Stampfli, G.M. & Hochard, C. (2009) Plate tectonics of the Alpine Realm. *Geological Society of London, Special Publication*, 327, 89–111.

Strasser, A. (1991) Lagoonal–peritidal sequences in carbonate environments: autocyclic and allocyclic processes. In: Einsele, G., Ricken, W. & Seilacher, A. (Eds.) *Cycles and events in stratigraphy*. Berlin: Springer, pp. 709–721.

Strasser, A. (1994) Meilankovitch cyclicity and high-resolution sequence stratigraphy in lagoonal–peritidal carbonates (Upper Tithonian–Lower Berriasian, French Jura Mountains). In: de Boer, P.L. & Smith, D.G. (Eds.) *Orbital forcing and cyclic sequences*, Vol. 19. Oxford, UK: IAS, Special Publication, pp. 285–301.

Strasser, A. (2018) Cyclostratigraphy of shallow-marine carbonates—limitations and opportunities. *Stratigraphy and Timescales*, 3, 151–187.

Strasser, A. & Davaud, E. (1983) Black pebbles of the Purbeckian (Swiss and French Jura): lithology, geochemistry and origin. *Eclogae Geologicae Helvetiae*, 76, 551–580.

Strasser, A., Hilgen, F.J. & Heckel, P.H. (2006) Cyclostratigraphy e concepts, definitions, and applications. *Newsletters on Stratigraphy*, 42, 75–114.

Strasser, A., Pittet, B., Hillgärtner, H. & Pasquier, J.B. (1999) Depositional sequences in shallow carbonate-dominated sedimentary systems: concepts for a high-resolution analysis. *Sedimentary Geology*, 128, 201–221.

Strasser, A., Hillgärtner, H., Hug, W. & Pittet, B. (2000) Third-order depositional sequences reflecting Milankovitch cyclicity. *Terra Nova*, 12, 303–311.

Tarling, D.H., Iorio, M. & D'Argenio, B. (1999) Geomagnetic long-term secular variations in Italian Lower Cretaceous shallow-water carbonates. *Geophysical Journal International*, 137(3), 713–722.

Tipper, J.C. (1997) Modeling carbonate platform sedimentation e lag comes naturally. *Geology*, 25, 495–498.

Tropeano, M., Caldara, A., De Santis, V., Festa, V., Parise, M., Sabato, L., Spalluto, L., Francescangeli, R., Iurilli, V., Mastronuzzi, G.A., Petruzzelli, M., Bellini, F., Cicala, M., Lippolis, M., Petti, F.M., Antonelli, M., Cardia, S., Conti, J., La Perna, R., Marino, M., Marsico, M., Sacco, E., Fiore, A., Simone, O., Valletta, S., D'Ettorre, U.S., De Giorgio, V., Liso, I.S. & Stigliano, E. (2023) Geological uniqueness and potential geoturistic appeal of Murge and Premurge, the first territory in Puglia (southern Italy) aspiring to become a UNESCO Global Geopark. *Geosciences*, 13, 131. https://doi.org/10.3390/geosciences13050131

Tucker, M.E. & Wright, V.P. (1990) *Carbonate sedimentology*. Oxford: Blackwell.

Vail, P.R., Audemard, F., Bowman, S.A., Eisner, P.N. & Perez Cruz, C. (1991) The stratigraphic signatures of Tectonics, Eustasy and sedimentology—an overview. In: Eisele, G., Rieken, W. & Seilacher, A. (Eds.) *Cycles and events in stratigraphy*. Berlin: Springer-Verlag, pp. 617–662.

Van Wagoner, J.C., Posamentier, H.W., Mitchum, R.M., Vail, P.R., Sarg, J.F., Loutit, T.S. & Hardenbol, L. (1988) An overwiev of the fundamentals of sequence stratigraphy and key definitions. In: Wilgus, C.K., Hastings, B.S., Kendall, C.G.S.C., Posamentier, H.W., Ross, C.A. & Van Wagoner, J.C. (Eds.) *Sea level changes: an integrated approach*, Vol. 42. Tulsa, Oklahoma, USA: SEPM, Special Publication, pp. 39–45.

Velić, I. (2007) Stratigraphy and palaeobiogeography of Mesozoic Benthic Foraminifera of the Karst Dinarides (SE Europa). *Geologia Croatica*, 60(1), 1–113.

Vlahovic, I., Tisljar, J., Velic, I. & Maticec, D. (2005) Evolution of the Adriatic carbonate platform: palaeogeography, main events and depositional dynamics. *Palaeogeography, Palaeoclimatology, Palaeoecology*, 220, 333–360.

Wilson, J.L. (1975) *Carbonate facies in geologic history*. Heidelberg: Springer-Verlag.

Wissler, L., Weissert, H., Buonocunto, F.P., Ferreri, V. & D'Argenio, B. (2004) Calibration of the Early Cretaceous time scale: a combined chemostratigraphic and cyclostratigraphic approach to the Barremian–Aptian interval, Campania Apennines and southern Alps. In: D'Argenio, B., Fischer, A.G., Premoli, S.I., Weissert, H. & Ferreri, V. (Eds.) *Cyclostratigraphy: approaches and case histories*, Vol. 81. Tulsa, Oklahoma, USA: SEPM, Special Publication, pp. 123–133.

Wright, V.P. (1994) Palaeosols in shallow marine carbonate sequences. *Earth-Science Reviews*, 35, 367–395.

Wright, V.P. (1996) Use of palaeosols in sequence stratigraphy of peritidal carbonates. In: Hesselbo, S.P. & Parkinson,

D.N. (Eds.) *Sequence stratigraphy in British Geology*, Vol. 103. London, UK: Geological Society of London Special Publication, pp. 63–74.

Zappaterra, E. (1990) Carbonate paleogeographic sequence of the Periadriatic region. *Bollettino della Societa Geologica Italiana*, 109, 5–20.

Zarcone, G., Petti, F.M., Cillari, A., Di Stefano, P., Guzzetta, D. & Nicosia, U. (2010) A possible bridge between Adria and Africa: new palaeobiogeographic and stratigraphic constraints on the Mesozoic palaeogeography of the Central Mediterranean area. *Earth Science Reviews*, 103, 154–162.

How to cite this article: Spalluto, L., Petruzzelli, M., Sabato, L. & Tropeano, M. (2024) Cretaceous cyclic peritidal carbonates of the Apulia Carbonate Platform (Apulia, southern Italy) in a hierarchical sequence-stratigraphic perspective: A case study from the Murge area (the Giovinazzo sea-cliff section). *The Depositional Record*, 00, 1–26. Available from: https://doi.org/10.1002/dep2.305